Nonlinear optimal control for permanent magnet synchronous spherical motors

Journal:	*Robotic Intelligence and Automation*
Manuscript ID	RIA-03-2023-0032.R2
Manuscript Type:	Original Article

Nonlinear optimal control for permanent magnet synchronous spherical motors

Abstract:

Purpose: Permanent magnet synchronous spherical motors can have wide use in robotics and industrial automation. They enable 3-DOF omnidirectional motion of their rotor. They are suitable for several applications as for instance actuation in robotics, traction in electric vehicles and use in several automation systems. Unlike conventional synchronous motors, permanent magnet synchronous spherical motors consist of a fixed inner shell which is the stator and a rotating outer shell which is the rotor. Their dynamic model is multivariable and strongly nonlinear. The treatment of the associated control problem is important.

Design/methodology/approach: In this article the multivariable dynamic model of permanent magnet synchronous spherical motors is analyzed and a nonlinear optimal (H-infinity) control method is developed for it. Differential flatness properties are proven for the spherical motor's state-space model. Next, the motor's state-space description undergoes approximate linearization with the use of first-order Taylor series expansion and through the computation of the associated Jacobian matrices. The linearization process takes place at each sampling instance around a time-varying operating point which is defined by the present value of the motors' state vector and by the last sampled value of the control inputs vector. For the approximately linearized model of the permanent magnet synchronous spherical motor a stabilizing H-infinity feedback controller is designed. To compute the controller's gains an algebraic Riccati equation has to be repetitively solved at each time-step of the control algorithm. The global stability properties of the control scheme are proven through Lyapunov analysis. Finally, the performance of the nonlinear optimal control method is compared against a flatness-based control approach implemented in successive loops.

Findings: Due to the nonlinear and multivariable structure of the state-space model of spherical motors the solution of the associated nonlinear control problem is a non-trivial task. In this article a novel nonlinear optimal (H-infinity) control approach is proposed for the dynamic model of permanent magnet synchronous spherical motors. The method is based on approximate linearization of the motor's state-space model with the use of first-order Taylor series expansion and through the computation of the associated Jacobian matrices. Furthermore, the article has introduced a different solution to the nonlinear control problem of the permanent magnet synchronous spherical motor which is based on flatness-based control implemented in successive loops.

Research limitations/implications: The presented control approaches do not exhibit any limitations but on the contrary they have specific advantages. In comparison to global linearization-based control schemes (such as Lie-algebra-based control) they do not make use of complicated changes of state variables (diffeomorphims) and transformations of the system's state-space description. The computed control inputs are applied directly on the initial nonlinear state-space model of the PM spherical motor without the intervention of inverse transformations and thus without coming against the risk of singularities.

Practical implications: The motion control problem of spherical motors is non-trivial because of the complicated nonlinear and multivariable dynamics of these electric machines. So far, there have been

several attempts to apply nonlinear feedback control to permanent magnet synchronous spherical motors. However, due to the model's complexity, few results exist about the associated nonlinear optimal control problem. The proposed nonlinear control method for permanent magnet synchronous spherical motors make more efficient, precise and reliable the use of such motors in robotics, in electric traction and in several automation systems

Social implications: The treated research topic is central for robotic and industrial automation. Permanent magnet synchronous spherical motors are suitable for several applications as for instance actuation in robotics, traction in electric vehicles and use in several automation systems. The solution of the control problem for the nonlinear dynamical model of permanent magnet synchronous spherical motors has many industrial applications and therefore contributes to economic growth and development.

Originality/value:The proposed nonlinear optimal control method is novel comparing to past attempts for solving the optimal control problem for nonlinear dynamical systems. Unlike past approaches, in the new nonlinear optimal control method linearization is performed around a temporary operating point which is defined by the present value of the system's state vector and by the last sampled value of the control inputs vector and not at points that belong to the desirable trajectory (setpoints). Besides, the Riccati equation which is used for computing the feedback gains of the controller is new, and so is the global stability proof for this control method. Comparing to NMPC (Nonlinear Model Predictive Control) which is a popular approach for treating the optimal control problem in industry, the new nonlinear optimal (H-infinity) control scheme is of proven global stability and the convergence of its iterative search for the optimum does not depend on initial conditions and trials with multiple sets of controller parameters. It is also noteworthy that the nonlinear optimal control method is applicable to a wider class of dynamical systems than approaches based on the solution of State Dependent Riccati Equations (SDRE). The SDRE approaches can be applied only to dynamical systems which can be transformed to the Linear Parameter Varying (LPV) form. Besides, the nonlinear optimal control method performs better than nonlinear optimal control schemes which use approximation of the solution of the Hamilton-Jacobi-Bellman equation by Galerkin series expansions. Furthermore. the second control method which is proposed by the article, that is flatness-based control loop is also novel, and demonstrates substantial contribution in nonlinear control for robotics and industrial automation.

Keywords: spherical motors, permanent magnent sychronous motors, nonlinear H-infinity control, Taylor series expansion, Jacobian matrices, Riccati equation, global stability, differential flatness properties, flatness-based control in successive loops.

1 Introduction

Permanent magnet synchronous spherical motors enable 3-DOF omnidirectional motion of their rotor (Bai et al., 2022), (Liu et al., 2017), (Bai and Lee, 2018). They are suitable for several applications as for instance actuation in robotics, traction in electric vehicles and use in several automation systems (Bai et al., 2021), (Bai et al., 2022), (Bai and Lee, 2014). Unlike conventional synchronous motors, permanent magnet synchronous spherical motors consist of a fixed inner shell which is the stator and a rotating outer shell which is the rotor (Bai et al., 2016), (Wen et al., 2021), (Li et al., 2020). The stator is supplied with a number of electromagnetic coils (EM) while the rotor is supplied with a number of permanent magnets (PM) grouped in pole pairs (Guo et al., 2019), (Rong et al., 2019), (Chai et al., 2020). Current circulates in the stator's electromagnetic coils and the interaction of the electromagnetic field of the stator's EMs with the magnetic field of the rotor's PMs generates the 3-DOF turn motion of the rotor (Sun and Lee, 2014), (Liu et al., 2017), (Chen et al., 2020). The dynamics of the rotor's turn motion is determined by Euler-Lagrange equations (Wen et al., 2022), (Rigatos, 2015a), (Rigatos and Karapanou, 2020). This dynamic model receives as control inputs three torque variables which determine rotation by a certain angle

around the axes of a cartesian coordinates frame (Xia et al., 2010), (Li et al., 2018), (Li et al., 2019). These mechanical torque variables are in turn associated with the currents of stator's EMs through an algebraic matrices relation (Yan et al., 2014), (Rossini et al., 2013), (Yan et al., 2010). Thus, the EMs currents are the final control inputs of the spherical motor (Gan et al., 2020), (Yan et al., 2006), (Wang et al., 2016). The motion control problem of spherical motors is non-trivial because of the complicated nonlinear and multivariable dynamics of these electric machines (Guo et al., 2020), (Liu et al., 2018), (Kumagui et al., 2013). So far, there have been several attempts to apply nonlinear feedback control to permanent magnet synchronous spherical motors (Zhang et al., 2016), (Guidan et al., 2011), (Lee and Sun, 2005). However, due to the model's complexity, few results exist about the associated nonlinear optimal control problem (Rigatos, 2016), (Chen et al., 2012), (Park et al., 2018). The application of spherical motors in drive systems can greatly simplify mechanical transmission components, improve torque density, efficiency and other performance indicators (Lee and Sun, 2023), (Ogulmuz and Tirkir, 2023), (Zhao et al., 2023), (Wen et al., 2023), (Zhou et al., 2023) . Therefore, they are expected to have broad application prospects in fields such as electric traction, robotics and aerospace (Huang et al., 2022), (Han et al., 2022).

In this article, a novel nonlinear optimal control method is proposed for the dynamic model of the permanent magnet synchronous spherical motor (Rigatos and Karapanou, 2020), (Rigatos, 2016). First, the state-space model of this actuation system is formulated in matrix form and its differential flatness properties are proven (Rigatos, 2015a). Next, the state-space model of the spherical motor undergoes a linearization procedure which takes place at each sampling instance around a temporary operating point which is updated at each time-step of the control algorithm. The linearization point is defined at each sampling interval by the present value of the motor's state vector and by the last sampled value of the control inputs vector. The linearization process is based on first-order Taylor series expansion and on the computation of the associated Jacobian matrices (Rigatos and Tzafestas, 2007), (Basseville and Nikiforov, 1993), (Rigatos and Zhang, 2009). The modelling error which is due to the truncation of higher-order terms in the Taylor series expansion is compensated by the robustness of the nonlinear optimal control algorithm. To select the controller's feedback gains an algebraic Riccati equation in repetitively solved at each time-step of the control method (Rigatos and Busawon, 2018), (Rigatos et al., 2022). The global stability properties of the control loop are proven through Lyapunov analysis (Rigatos, 2016), (Rigatos et al., 2015), (Toussaint et al., 2000).

Next, flatness-based control in successive loops is also developed for the dynamic model of the permanent magnet synchronous spherical motor (Rigatos et al., 2018), (Rigatos, 2015b). The method of flatness-based control in successive loops was first introduced in (Rigatos, 2015a). The dynamic model of the spherical motor is separated into two subsystems, where the first subsystem has as state variables the turn angles of the rotor around the reference axes of a cartesian coordinates frame, while the second subsystem has as state variables the associated angular velocities. Each one of these subsystems can be viewed independently as a differentially flat system and control about it can be performed with inversion of its dynamics as in the case of input-output linearized flat systems. The state variables of the second subsystem (angular velocities of the rotor) become virtual control inputs for the first subsystem (turn angles of the rotor). Finally, exogenous control inputs are applied to the second subsystem (torques that modify the angular speed of the rotor). The whole control method is implemented in two successive loops and its global stability properties are also proven through Lyapunov stability analysis.

The structure of the article is as follows: in Section 2 the dynamic model of the permanent magnet synchronous spherical motor is given in state-space form and its differential flatness properties are proven. Morover, the relation that connects the mechanical torques of the rotor with the currents of the stator's EMs is given. In Section 3 the state-space model of the spherical motor undergoes approximate linearization with first-order Taylor series expansion and through the computation of the associated Jacobian matrices. In Section 4 the solution of the nonlinear optimal control problem for the spherical motor is provided and the associated Lyapunov stability analysis is given. In Section 5 a flatness-based controller is successive

loop is formulated for the dynamic model of the spherical motor. In Section 6 the performance of the nonlinear optimal control is tested through simulation experiments and is compared against a flatness -based controller in successive loops for the dynamic model of the spherical motor. Finally, in Section 7 concluding remarks are stated.

2 Dynamic model of the permanent magnet spherical motor

2.1 State-space model of the spherical motor

The diagram of the 3-DOF spherical motor and the associated coordinate frames about the rotor's motion are shown in Fig. 1. The outer shell of the motor is the rotor and has permanent magnets on it. The inner part of the motor is the stator and is supplied with electromagnets. The interaction between the stator's electromagnets and the rotor's permanent magnets generates the torque which enables 3-DOF rotations for the rotor (Bai et al., 2022), (Liu et al., 2017), (Bai and Lee, 2018).

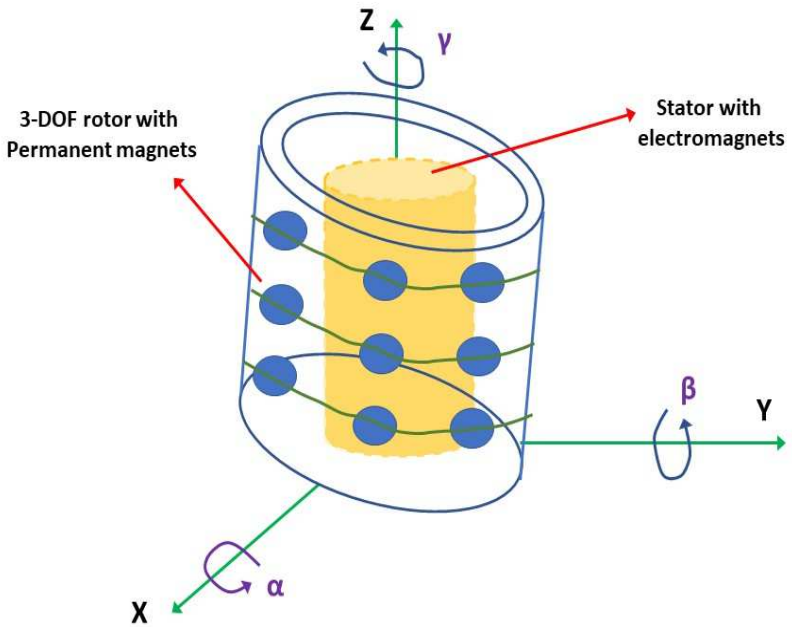

Figure 1: Diagram of the 3-DOF spherical synchronous motor with permanent magnets at the rotor (Source: Authors' own work)

The vector of the turn angles of the rotor around the axes of the inertial reference frame is given by $q = [\alpha, \beta, \gamma]^T$. The vector of the associated angular velocities is given by $\dot{q} = [\dot{\alpha}, \dot{\beta}, \dot{\gamma}]^T$. Using Euler-Lagrange analysis one obtains the dynamic model of the spherical motor. This is given by (Bai et al., 2022)

$$M(q)\ddot{q} + C(q, \dot{q})\dot{q} + G(q) = \tau - \tau_d \tag{1}$$

where the inertia matrix is given by

$$M(q) = \begin{pmatrix} I_a cos(\beta)^2 + I_t sin(\beta)^2 + m h_z^2 cos(\beta)^2 & 0 & I_t sin(\beta) \\ 0 & I_a + m h_z^2 & 0 \\ I_t sin(\beta) & 0 & I_t \end{pmatrix} \quad (2)$$

and the Coriolis-centrifugal forces matrix is given by

$$C(q,\dot{q})\dot{q} = \begin{pmatrix} 2\dot{\alpha}\dot{\beta} cos(\beta) sin(\beta) I_a + 2\dot{\alpha}\dot{\beta} sin(\beta) cos(\beta)(I_z - m h_z^2) + I_t \dot{\beta}\dot{\gamma} cos(\beta) \\ \dot{\alpha}^2 sin(\gamma) cos(\beta)(I_a + m h_z^2 - I_t) - I_t \dot{\alpha}\dot{\gamma} cos(\beta) \\ I_t \dot{\alpha}\dot{\beta} cos(\beta) \end{pmatrix} \quad (3)$$

The gravitational forces vector and the disturbance torques vector are given by

$$G(q) = m g h_z \begin{pmatrix} -cos(\beta) sin(\alpha) \\ -sin(\beta) cos(\alpha) \\ 0 \end{pmatrix} \quad \tau_d = \begin{pmatrix} b_1 \dot{\alpha} \\ b_2 \dot{\beta} \\ b_3 \dot{\gamma} \end{pmatrix} \quad (4)$$

As noted above, in the dynamic model of the spherical permanent magnet motor of Eq. (1) $M(q)$ is the inertia matrix which is symmetric and positive definite, $C(q,\dot{q})\dot{q}$ is the Coriolis and centrifugal forces matrix and $G(q)$ is the gravitational forces matrix. Moreover, I_a is the moment of inertia for rotation around the X and Y axis and I_t is the moment of inertia for rotation around the Z axis. Other parameters of the model are: m which is the mass of the rotor, and h_z which is the distance between the center of the mass and the center of rotation. Finally, τ is the motor's electromagnetic torque which is generated by the interaction between the stator's electromagnets and the rotor's permanent magnets, while τ_d is the disturbance torques vector (Bai et al., 2022).

The inverse of the inertia matrix $M(q)$ is given by

$$M(q)^{-1} = \frac{1}{detM} \begin{pmatrix} M_{11} & -M_{21} & M_{31} \\ -M_{12} & M_{22} & -M_{32} \\ M_{13} & -M_{23} & M_{33} \end{pmatrix} \quad (5)$$

where the determinant $detM$ is given by $detM = I_t(I_a + h_z^2)[I_a cos(\beta)^2 + m h_z^2 cos(\beta)^2]$. The sub-determinant of matrix M are defined as follows: $M_{11} = I_t(I_a + m h_z^2)$, $M_{12} = 0$, $M_{13} = -(I_t) sin(\beta)(I_a + m h_z^2)$, $M_{21} = 0$, $M_{22} = (I_a + m h_z^2) I_t cos(\beta)^2$, $M_{23} = 0$, $M_{31} = (I_a + m h_z^2) I_t sin(\beta)$, $M_{32} = 0$ and $M_{33} = [I_a cos(\beta)^2 + I_t sin(\beta)^2 + m h_z^2 cos(\beta)^2](I_a + m h_z^2)$.

Using the inverse of the inertia matrix $M(q)$ and Eq. (1) the dynamic model of the permanent magnet spherical motor becomes

$$\ddot{q} = -M(q)^{-1} C(q,\dot{q})\dot{q} - M(q)^{-1} g(q) - M(q)^{-1}\tau_d + M(q)^{-1}\tau \quad (6)$$

Eq. (6) can be also written analytically as

$$\begin{pmatrix} \ddot{\alpha} \\ \ddot{\beta} \\ \ddot{\gamma} \end{pmatrix} = -\frac{1}{detM} \begin{pmatrix} M_{11} & -M_{21} & M_{31} \\ -M_{12} & M_{22} & -M_{32} \\ M_{13} & -M_{23} & M_{33} \end{pmatrix} \begin{pmatrix} C_1 + G_1 + \tau_{d_1} \\ C_2 + G_2 + \tau_{d_2} \\ C_3 + G_3 + \tau_{d_3} \end{pmatrix} + \frac{1}{detM} \begin{pmatrix} M_{11} & -M_{21} & M_{31} \\ -M_{12} & M_{22} & -M_{32} \\ M_{13} & -M_{23} & M_{33} \end{pmatrix} \begin{pmatrix} \tau_1 \\ \tau_2 \\ \tau_3 \end{pmatrix} \quad (7)$$

or equivalently

$$\begin{pmatrix}\ddot{\alpha}\\ \ddot{\beta}\\ \ddot{\gamma}\end{pmatrix}=\begin{pmatrix}\frac{-M_{11}(C_1+G_1+\tau_{d1})+M_{21}(C_2+G_2+\tilde{d}_2)-M_{31}(C_3+G_3+\tau_{d3})}{detM}\\ \frac{M_{12}(C_1+G_1+\tau_{d1})-M_{22}(C_2+G_2+\tilde{d}_2)+M_{32}(C_3+G_3+\tau_{d3})}{detM}\\ \frac{-M_{13}(C_1+G_1+\tau_{d1})+M_{23}(C_2+G_2+\tilde{d}_2)-M_{33}(C_3+G_3+\tau_{d3})}{detM}\end{pmatrix}+\begin{pmatrix}\frac{M_{11}}{detM} & -\frac{M_{21}}{detM} & \frac{M_{31}}{detM}\\ -\frac{M_{12}}{detM} & \frac{M_{22}}{detM} & -\frac{M_{32}}{detM}\\ \frac{M_{13}}{detM} & -\frac{M_{23}}{detM} & \frac{M_{33}}{detM}\end{pmatrix}\begin{pmatrix}\tau_1\\ \tau_2\\ \tau_3\end{pmatrix} \tag{8}$$

The state vector of the spherical permanent magnets motor is $x=[x_1,x_2,x_3,x_4,x_5,x_6]^T$ or equivalently $x=[\alpha,\dot{\alpha},\beta,\dot{\beta},\gamma,\dot{\gamma}]^T$. The control inputs vector of the system is $u=[u_1,u_2,u_3]^T$ or equivalently $u=[\tau_1,\tau_2,\tau_3]^T$.

Using the state variables notation the determinant and the sub-determinants of the inertia matrix are written as follows: $detM=I_t(I_a+h_z^2)[I_acos(\beta)^2+mh_z^2cos(\beta)^2]$. The sub-determinant of matrix M are defined as follows: $M_{11}=I_t(I_a+mh_z^2)$, $M_{12}=0$, $M_{13}=-(I_t)sin(x_3)(I_a+mh_z^2)$, $M_{21}=0$, $M_{22}=(I_a+mh_z^2)I_tcos(x_3)^2$, $M_{23}=$, $M_{31}=(I_a+mh_z^2)I_tsin(x_3)$, $M_{32}=0$ and $M_{33}=[I_acos(x_3)^2+I_tsin(x_3)^2+mh_z^2cos(x_3)^2](I_a+mh_z^2)$.

Additionally, about the elements of the Coriolis matrix one has: $C_1=2\dot{a}\dot{\beta}cos(\beta)sin(\beta)I_a+2\dot{a}\dot{\beta}sin(\beta)cos(\beta)(I_z-mh_z^2)+I_t\dot{\beta}\dot{\gamma}cos(\beta)$, $C_2=\dot{a}^2sin(\gamma)cos(\beta)(I_a+mh_z^2-I_t)-I_t\dot{a}\dot{\gamma}cos(\beta)$ and $C_3=I_t\dot{a}\dot{\beta}cos(\beta)$.

Moreover, about the elements of the gravitational vector and about the elements of the disturbance torque vector one has: $G_1=-mgh_zcos(x_3)sin(x_1)$, $G_2=-mgh_zsin(x_3)cos(x_1)$, $G_3=0$ and $\tau_{d1}=b_2x_2$, $\tau_{d2}=b_2x_4$, $\tau_{d3}=b_3x_6$

Consequently, the state-space model of the spherical motor is written in the following matrix form

$$\begin{pmatrix}\dot{x}_1\\ \dot{x}_2\\ \dot{x}_3\\ \dot{x}_4\\ \dot{x}_5\\ \dot{x}_6\end{pmatrix}=\begin{pmatrix}x_2\\ \frac{-M_{11}(C_1+G_1+\tau_{d1})+M_{21}(C_2+G_2+\tilde{d}_2)-M_{31}(C_3+G_3+\tau_{d3})}{detM}\\ x_4\\ \frac{M_{12}(C_1+G_1+\tau_{d1})-M_{22}(C_2+G_2+\tilde{d}_2)+M_{32}(C_3+G_3+\tau_{d3})}{detM}\\ x_6\\ \frac{-M_{13}(C_1+G_1+\tau_{d1})+M_{23}(C_2+G_2+\tilde{d}_2)-M_{33}(C_3+G_3+\tau_{d3})}{detM}\end{pmatrix}+\begin{pmatrix}0 & 0 & 0\\ \frac{M_{11}}{detM} & -\frac{M_{21}}{detM} & \frac{M_{31}}{detM}\\ 0 & 0 & 0\\ -\frac{M_{12}}{detM} & \frac{M_{22}}{detM} & -\frac{M_{32}}{detM}\\ 0 & 0 & 0\\ \frac{M_{13}}{detM} & -\frac{M_{23}}{detM} & \frac{M_{33}}{detM}\end{pmatrix}\begin{pmatrix}u_2\\ u_2\\ u_3\end{pmatrix} \tag{9}$$

The state-space model of the spherical motor given in Eq. (9) can be also written in the following concise nonlinear affine-in-the-input state-space form:

$$\dot{x}=f(x)+g(x)u \tag{10}$$

where $x\in R^{6\times1}$, $f(x)\in R^{6\times1}$, $g(x)\in R^{6\times3}$ and $u\in R^{3\times1}$.

2.2 Computation of the electromagnetic torque of the spherical motor

The minimum torque model is established with the use of the characteristic function of the torque which is developed between a permanent magnet (PM) pole at the rotor and an electromagnetic (EM) coil at the stator of the spherical motor. This model makes use of the so-called *separation angle* while the *characteristic function* is computed with the use of the finite-elements method. Thus, the minimum torque model between the i-th stator coil and the j-th permanent magnet pole is given by

$$\tau_{ij}=f(\theta_{ij})\frac{x_{si}\times x_{rj}}{|x_{si}\times x_{rj}|} \tag{11}$$

where θ_{ij} is the separation angle between the i-th EM coil of the stator $i = 1, 2, \cdots, N_{em}$ and the j-th PM of the rotor $j = 1, 2, \cdots, N_{pm}$. Moreover, I_i is the current at the i-th EM coil and all such currents form the real control inputs vector of the motor. Furthermore, $x_{si} \in R^3$ is a vector defining the position of the i-th EM of the stator in a cartesian coordinates frame while $x_{rj} \in R^3$ is a vector defining the position of the j-th PM of the rotor in this coordinates frame. The torque element τ_{ij} represents the electromagnetic torque generated between the i-th EM coil of the stator and the j-th PM pole of the rotor. According to the above, the cumulative torque vector, consisting of three cartesian components τ_x, τ_y, τ_z, is given by

$$\tau = \sum_{i=1}^{N_{em}} \sum_{j=1}^{N_{pm}} f(\theta_{ij}) \frac{x_{si} \times x_{rj}}{|x_{si} \times x_{rj}|} \tag{12}$$

The relation about the cumulative electromagnetic torque of the rotor is given by

$$\tau = \begin{pmatrix} \tau_x \\ \tau_y \\ \tau_z \end{pmatrix} = \begin{pmatrix} q_{x,1} & q_{x,2} & \cdots & q_{x,N_{em}} \\ q_{y,1} & q_{y,2} & \cdots & q_{y,N_{em}} \\ q_{z,1} & q_{z,2} & \cdots & q_{z,N_{em}} \end{pmatrix} \begin{pmatrix} I_1 \\ I_2 \\ \cdots \\ I_{N_{em}} \end{pmatrix} \tag{13}$$

where coefficient $q_{x,i}$, $i = 1, 2, \cdots, N_{em}$ is obtained by summing up all x-axis components of the torque elements τ_{ij} for $j = 1, 2, \cdots, N_{pm}$ which have been generated at the PMs of the rotor due to the current I_i at the i-th EM coil of the stator. Equivalently, coefficient $q_{y,i}$, $i = 1, 2, \cdots, N_{em}$ is obtained by summing up all y-axis components of the torque elements τ_{ij} for $j = 1, 2, \cdots, N_{pm}$ which have been generated at the PMs of the rotor due to the current I_i at the i-th EM coil of the stator. Finally, coefficient $q_{z,i}$, $i = 1, 2, \cdots, N_{em}$ is obtained by summing up all z-axis components of the torque elements τ_{ij} for $j = 1, 2, \cdots, N_{pm}$ which have been generated at the PMs of the rotor due to the current I_i at the i-th EM coil of the stator.

The above relation can be also written in the concise form

$$\tau = Q \cdot I \tag{14}$$

where $\tau \in R^{3\times 1}$, $Q \in R^{3\times N_{em}}$ and $I \in R^{N_{em}\times 1}$. Once the torque's vector $\tau = [\tau_x, \tau_y, \tau_z]^T$ which is associated with a specific rotational motion of the motor is given, one can compute the vector of currents of the EM coils of the stator which constitute the real control input vector of the motor. This is done using the pseudo-inverse matrix and the relation

$$I = [Q^T Q]^{-1} Q^T \cdot \tau \tag{15}$$

2.3 Differential flatness properties of the spherical motor

It will be proven that the dynamic model of the spherical motor is differentially flat with flat outputs vector $Y = [x_1, x_3, x_5]^T$ that is $Y = [\alpha, \beta, \gamma]^T$ (Rigatos, 2015a). The state-space model of the spherical motor is rewritten as

$$\begin{pmatrix} \dot{x}_1 \\ \dot{x}_2 \\ \dot{x}_3 \\ \dot{x}_4 \\ \dot{x}_5 \\ \dot{x}_6 \end{pmatrix} = \begin{pmatrix} x_2 \\ f_2(x) \\ x_4 \\ f_4(x) \\ x_6 \\ f_6(x) \end{pmatrix} + \begin{pmatrix} 0 & 0 & 0 \\ g_{12}(x) & g_{22}(x) & g_{32}(x) \\ 0 & 0 & 0 \\ g_{14}(x) & g_{24}(x) & g_{34}(x) \\ 0 & 0 & 0 \\ g_{16}(x) & g_{26}(x) & g_{36}(x) \end{pmatrix} \begin{pmatrix} u_1 \\ u_2 \\ u_3 \end{pmatrix} \tag{16}$$

Form the 1st, 3rd and 5th rows of the state-space model one has

$$x_2 = \dot{x}_1 \quad x_4 = \dot{x}_3 \quad x_6 = \dot{x}_5 \tag{17}$$

Consequently, state variables x_2, x_4 and x_6 are differential functions of the flat outputs of the system, or

$$x_2 = h_2(Y, \dot{Y}) \quad x_4 = h_4(Y, \dot{Y}) \quad x_6 = h_6(Y, \dot{Y}) \tag{18}$$

Besides, from the 2nd, 4th and 6th rows of the state-space model one has

$$\begin{pmatrix} \ddot{x}_1 \\ \ddot{x}_3 \\ \ddot{x}_5 \end{pmatrix} = \begin{pmatrix} f_2(x) \\ f_4(x) \\ f_6(x) \end{pmatrix} + \begin{pmatrix} g_{12}(x) & g_{22}(x) & g_{32}(x) \\ g_{14}(x) & g_{24}(x) & g_{34}(x) \\ g_{16}(x) & g_{26}(x) & g_{36}(x) \end{pmatrix} \begin{pmatrix} u_1 \\ u_2 \\ u_3 \end{pmatrix} \tag{19}$$

which finally gives

$$\begin{pmatrix} u_1 \\ u_2 \\ u_3 \end{pmatrix} = \begin{pmatrix} g_{12}(x) & g_{22}(x) & g_{32}(x) \\ g_{14}(x) & g_{24}(x) & g_{34}(x) \\ g_{16}(x) & g_{26}(x) & g_{36}(x) \end{pmatrix}^{-1} \left[\begin{pmatrix} \ddot{x}_1 \\ \ddot{x}_3 \\ \ddot{x}_5 \end{pmatrix} - \begin{pmatrix} f_2(x) \\ f_4(x) \\ f_6(x) \end{pmatrix} \right] \tag{20}$$

Consequently, the control inputs u_1, u_2 and u_3 are differential functions of the flat outputs of the system, or

$$u_1 = h_{u_1}(Y, \dot{Y}) \quad u_2 = h_{u_2}(Y, \dot{Y}) \quad u_3 = h_{u_3}(Y, \dot{Y}) \tag{21}$$

As a result of the above, the dynamic model of the permanent magnet synchronous motor is differentially flat. The differential flatness properties of the spherical motor demonstrate that: (i) the system can be transformed into an input-output linearized form through successive differentiations of its flat outputs, (ii) the setpoints definition problem for this system can be efficiently solved. One defines first setpoints without any constraints for state variables x_1, x_3, x_5 which are associated with the flat outputs of the system. Next, setpoints for x_2, x_4, x_6 are defined as differential functions of the setpoints for state variables x_1, x_3 and x_5.

3 Approximate linearization of the dynamic model of the spherical motor

3.1 The approximate linearization concept

The dynamic model of the spherical motor being initially in the state-space form of Eq. (10) undergoes approximate linearization, which allows for obtaining the equivalent state-space form

$$\dot{x} = Ax + Bu + \tilde{d} \tag{22}$$

where A, B are the Jacobian matrices of the nonlinear system and $\tilde{d}$ is the cumulative disturbance vector. The linearization process takes place at each sampling instance around the time-varying point (x^*, u^*) where x^* is the present value of the motor's state vector and u^* is the last sampled value of the control inputs vector. The linearization relies on first-order Taylor series expansion and on the computation of the associated Jacobian matrices. The modelling error $\tilde{d}$ may comprise (i) model uncertainty due to truncation of of higher-order terms in the Taylor series expansion (ii) exogenous perturbations, (iii) sensors measurement noise of any distribution.

Matrices A and B are the Jacobian matrices of the system which are computed as follows:

$$\begin{gathered} A = \nabla_x [f(x) + g(x)u] \mid_{(x^*, u^*)} \Rightarrow \\ A = \nabla_x [f(x)] \mid_{(x^*, u^*)} + \nabla_x [g_1(x)u_1] \mid_{(x^*, u^*)} + \nabla_x [g_2(x)u_2] \mid_{(x^*, u^*)} + \nabla_x [g_3(x)u_3] \mid_{(x^*, u^*)} \end{gathered} \tag{23}$$

$$B = \nabla_u [f(x) + g(x)u] \mid_{(x^*, u^*)} \Rightarrow B = g(x) \mid_{(x^*, u^*)} \tag{24}$$

The linearization approach which has been followed for implementing the nonlinear optimal control scheme results into a quite accurate model of the system's dynamics. Consider for instance the following affine-in-the-input state-space model

$$\dot{x} = f(x) + g(x)u \Rightarrow$$
$$\dot{x} = [f(x^*) + \nabla_x f(x)\mid_{x^*}(x - x^*)] + [g(x^*) + \nabla_x g(x)\mid_{x^*}(x - x^*)]u^* + g(x^*)u^* + g(x^*)(u - u^*) + \tilde{d}_1 \Rightarrow$$
$$\dot{x} = [\nabla_x f(x)\mid_{x^*} + \nabla_x g(x)\mid_{x^*} u^*]x + g(x^*)u - [\nabla_x f(x)\mid_{x^*} + \nabla_x g(x)\mid_{x^*} u^*]x^* + f(x^*) + g(x^*)u^* + \tilde{d}_1 \quad (25)$$

where $\tilde{d}_1$ is the modelling error due to truncation of higher order terms in the Taylor series expansion of $f(x)$ and $g(x)$. Next, by defining $A = [\nabla_x f(x)\mid_{x^*} + \nabla_x g(x)\mid_{x^*} u^*]$, $B = g(x^*)$ one obtains

$$\dot{x} = Ax + Bu - Ax^* + f(x^*) + g(x^*)u^* + \tilde{d}_1 \quad (26)$$

Moreover by denoting $\tilde{d} = -Ax^* + f(x^*) + g(x^*)u^* + \tilde{d}_1$ about the cumulative modelling error term in the Taylor series expansion procedure one has

$$\dot{x} = Ax + Bu + \tilde{d} \quad (27)$$

which is the approximately linearized model of the dynamics of the system of Eq. (22). The term $f(x^*) + g(x^*)u^*$ is the derivative of the state vector at (x^*, u^*) which is almost annihilated by $-Ax^*$.

3.2 Computation of Jacobian matrices

The computation of the Jacobian matrix $A = \nabla_x[f(x)]\mid_{(x^*,u^*)}$ proceeds as follows:

First row of the Jacobian matrix $A = \nabla_x[f(x)]\mid_{(x^*,u^*)}$: $\frac{\partial f_1}{\partial x_1} = 0$, $\frac{\partial f_1}{\partial x_2} = 1$, $\frac{\partial f_1}{\partial x_3} = 0$, $\frac{\partial f_1}{\partial x_4} = 0$, $\frac{\partial f_1}{\partial x_5} = 0$, $\frac{\partial f_1}{\partial x_6} = 0$.

Second row of the Jacobian matrix $A = \nabla_x[f(x)]\mid_{(x^*,u^*)}$: It holds that $f_2(x) = \frac{f_{2,num}(x)}{f_{2,den}(x)}$ where $f_{2,num}(x) = -M_{11}(C_1 + G_1 + \tau_{d1}) + M_{21}(C_2 + G_2 + \tau_{d2}) - M_{31}(C_3 + G_3 + \tau_{d3})$ and $f_{2,den}(x) = detM$. Thus

$$\frac{\partial f_2(x)}{\partial x_i} = \frac{\frac{\partial f_{2,num}}{\partial x_i} f_{2,den} - f_{2,num}\frac{\partial f_{2,den}}{\partial x_i}}{f_{2,den}^2} \quad (28)$$

where for $i = 1, 2, 3, 4, 5, 6$

$$\begin{aligned}\frac{\partial f_{2,num}(x)}{\partial x_i} = &-\frac{\partial M_{11}}{\partial x_i}(C_1 + G_1 + \tau_{d1}) - M_{11}(\frac{\partial C_1}{\partial x_i} + \frac{\partial G_1}{\partial x_i} + \frac{\partial \tau_{d1}}{\partial x_i}) + \\ &+\frac{\partial M_{21}}{\partial x_i}(C_2 + G_2 + \tau_{d2}) + M_{21}(\frac{\partial C_2}{\partial x_i} + \frac{\partial G_2}{\partial x_i} + \frac{\partial \tau_{d2}}{\partial x_i}) - \\ &-\frac{\partial M_{31}}{\partial x_i}(C_1 + G_2 + \tau_{d1}) - M_{31}(\frac{\partial C_3}{\partial x_i} + \frac{\partial G_3}{\partial x_i} + \frac{\partial \tau_{d3}}{\partial x_i})\end{aligned} \quad (29)$$

and for $i = 1, 2, 3, 4, 5, 6$

$$\frac{\partial f_{2,den}(x)}{\partial x_i} = \frac{\partial detM}{\partial x_i} \quad (30)$$

Third row of the Jacobian matrix $A = \nabla_x[f(x)]\mid_{(x^*,u^*)}$: $\frac{\partial f_3}{\partial x_1} = 0$, $\frac{\partial f_3}{\partial x_2} = 0$, $\frac{\partial f_3}{\partial x_3} = 0$, $\frac{\partial f_3}{\partial x_4} = 1$, $\frac{\partial f_3}{\partial x_5} = 0$, $\frac{\partial f_3}{\partial x_6} = 0$.

Fourth row of the Jacobian matrix $A = \nabla_x[f(x)]\mid_{(x^*,u^*)}$: It holds that $f_4(x) = \frac{f_{4,num}(x)}{f_{4,den}(x)}$ where $f_{4,num}(x) = M_{12}(C_1 + G_1 + \tau_{d1}) - M_{22}(C_2 + G_2 + \tau_{d2}) + M_{32}(C_3 + G_3 + \tau_{d3})$ and $f_{4,den}(x) = detM$. Thus

$$\frac{\partial f_4(x)}{\partial x_i} = \frac{\frac{\partial f_{4,num}}{\partial x_i} f_{4,den} - f_{4,num}\frac{\partial f_{4,den}}{\partial x_i}}{f_{4,den}^2} \quad (31)$$

where for $i = 1, 2, 3, 4, 5, 6$

$$\frac{\partial f_{4,num}(x)}{\partial x_i} = \frac{\partial M_{12}}{\partial x_i}(C_1 + G_1 + \tau_{d1}) + M_{12}(\frac{\partial C_1}{\partial x_i} + \frac{\partial G_1}{\partial x_i} + \frac{\partial \tau_{d1}}{\partial x_i}) + \\ - \frac{\partial M_{22}}{\partial x_i}(C_2 + G_2 + \tau_{d2}) - M_{22}(\frac{\partial C_2}{\partial x_i} + \frac{\partial G_2}{\partial x_i} + \frac{\partial \tau_{d2}}{\partial x_i}) + \\ + \frac{\partial M_{32}}{\partial x_i}(C_1 + G_2 + \tau_{d1}) + M_{32}(\frac{\partial C_3}{\partial x_i} + \frac{\partial G_3}{\partial x_i} + \frac{\partial \tau_{d3}}{\partial x_i}) \tag{32}$$

and for $i = 1, 2, 3, 4, 5, 6$

$$\frac{\partial f_{4,den}(x)}{\partial x_i} = \frac{\partial detM}{\partial x_i} \tag{33}$$

Fifth row of the Jacobian matrix $A = \nabla_x[f(x)] \mid_{(x^*,u^*)}$: $\frac{\partial f_5}{\partial x_1} = 0$, $\frac{\partial f_5}{\partial x_2} = 0$, $\frac{\partial f_5}{\partial x_3} = 0$, $\frac{\partial f_5}{\partial x_4} = 0$, $\frac{\partial f_5}{\partial x_5} = 0$, $\frac{\partial f_5}{\partial x_6} = 1$.

Sixth row of the Jacobian matrix $A = \nabla_x[f(x)] \mid_{(x^*,u^*)}$: It holds that $f_6(x) = \frac{f_{6,num}(x)}{f_{6,den}(x)}$ where $f_{6,num}(x) = -M_{13}(C_1 + G_1 + \tau_{d1}) + M_{23}(C_2 + G_2 + \tau_{d2}) - M_{33}(C_3 + G_3 + \tau_{d3})$ and $f_{6,den}(x) = detM$. Thus

$$\frac{\partial f_6(x)}{\partial x_i} = \frac{\frac{\partial f_{6,num}}{\partial x_i} f_{6,den} - f_{6,num} \frac{\partial f_{6,den}}{\partial x_i}}{f_{6,den}^2} \tag{34}$$

where for $i = 1, 2, 3, 4, 5, 6$

$$\frac{\partial f_{6,num}(x)}{\partial x_i} = -\frac{\partial M_{13}}{\partial x_i}(C_1 + G_1 + \tau_{d1}) - M_{13}(\frac{\partial C_1}{\partial x_i} + \frac{\partial G_1}{\partial x_i} + \frac{\partial \tau_{d1}}{\partial x_i}) + \\ + \frac{\partial M_{23}}{\partial x_i}(C_2 + G_2 + \tau_{d2}) + M_{23}(\frac{\partial C_2}{\partial x_i} + \frac{\partial G_2}{\partial x_i} + \frac{\partial \tau_{d2}}{\partial x_i}) - \\ - \frac{\partial M_{33}}{\partial x_i}(C_1 + G_2 + \tau_{d1}) - M_{33}(\frac{\partial C_3}{\partial x_i} + \frac{\partial G_3}{\partial x_i} + \frac{\partial \tau_{d3}}{\partial x_i}) \tag{35}$$

and for $i = 1, 2, 3, 4, 5, 6$

$$\frac{\partial f_{6,den}(x)}{\partial x_i} = \frac{\partial detM}{\partial x_i} \tag{36}$$

Computation of the Jacobian matrix $\nabla_x g_1(x) \mid_{(x^*,u^*)}$:

It holds that $g_{21}(x) = \frac{M_{11}}{detM}$ thus for $i = 1, 2, 3, 4, 5, 6$

$$\frac{\partial g_{21}}{\partial x_i} = \frac{\frac{\partial M_{11}}{\partial x_i} detM - M_{11} \frac{\partial detM}{\partial x_i}}{detM^2} \tag{37}$$

Moreover $g_{41}(x) = -\frac{M_{12}}{detM}$ thus for $i = 1, 2, 3, 4, 5, 6$

$$\frac{\partial g_{41}}{\partial x_i} = -\frac{\frac{\partial M_{12}}{\partial x_i} detM - M_{12} \frac{\partial detM}{\partial x_i}}{detM^2} \tag{38}$$

Additionally $g_{61}(x) = \frac{M_{13}}{detM}$ thus for $i = 1, 2, 3, 4, 5, 6$

$$\frac{\partial g_{61}}{\partial x_i} = \frac{\frac{\partial M_{13}}{\partial x_i} detM - M_{13} \frac{\partial detM}{\partial x_i}}{detM^2} \tag{39}$$

Consequently

$$\nabla_x g_1(x) \mid_{(x^*,u^*)} = \begin{pmatrix} 0 & 0 & 0 & 0 & 0 & 0 \\ \frac{\partial g_{21}(x)}{\partial x_1} & \frac{\partial g_{21}(x)}{\partial x_2} & \frac{\partial g_{21}(x)}{\partial x_3} & \frac{\partial g_{21}(x)}{\partial x_4} & \frac{\partial g_{21}(x)}{\partial x_5} & \frac{\partial g_{21}(x)}{\partial x_6} \\ 0 & 0 & 0 & 0 & 0 & 0 \\ \frac{\partial g_{41}(x)}{\partial x_1} & \frac{\partial g_{41}(x)}{\partial x_2} & \frac{\partial g_{41}(x)}{\partial x_3} & \frac{\partial g_{41}(x)}{\partial x_4} & \frac{\partial g_{41}(x)}{\partial x_5} & \frac{\partial g_{41}(x)}{\partial x_6} \\ 0 & 0 & 0 & 0 & 0 & 0 \\ \frac{\partial g_{61}(x)}{\partial x_1} & \frac{\partial g_{61}(x)}{\partial x_2} & \frac{\partial g_{61}(x)}{\partial x_3} & \frac{\partial g_{61}(x)}{\partial x_4} & \frac{\partial g_{61}(x)}{\partial x_5} & \frac{\partial g_{61}(x)}{\partial x_6} \end{pmatrix} \tag{40}$$

Computation of the Jacobian matrix $\nabla_x g_2(x) \mid_{(x^*,u^*)}$:

It holds that $g_{22}(x) = -\frac{M_{21}}{detM}$ thus for $i = 1, 2, 3, 4, 5, 6$

$$\frac{\partial g_{22}}{\partial x_i} = -\frac{\frac{\partial M_{21}}{\partial x_i} detM - M_{21}\frac{\partial detM}{\partial x_i}}{detM^2} \tag{41}$$

Moreover $g_{42}(x) = \frac{M_{12}}{detM}$ thus for $i = 1, 2, 3, 4, 5, 6$

$$\frac{\partial g_{42}}{\partial x_i} = \frac{\frac{\partial M_{22}}{\partial x_i} detM - M_{22}\frac{\partial detM}{\partial x_i}}{detM^2} \tag{42}$$

Additionally $g_{62}(x) = -\frac{M_{23}}{detM}$ thus for $i = 1, 2, 3, 4, 5, 6$

$$\frac{\partial g_{62}}{\partial x_i} = -\frac{\frac{\partial M_{23}}{\partial x_i} detM - M_{23}\frac{\partial detM}{\partial x_i}}{detM^2} \tag{43}$$

Consequently

$$\nabla_x g_2(x) \mid_{(x^*,u^*)} = \begin{pmatrix} 0 & 0 & 0 & 0 & 0 & 0 \\ \frac{\partial g_{22}(x)}{\partial x_1} & \frac{\partial g_{22}(x)}{\partial x_2} & \frac{\partial g_{22}(x)}{\partial x_3} & \frac{\partial g_{22}(x)}{\partial x_4} & \frac{\partial g_{22}(x)}{\partial x_5} & \frac{\partial g_{22}(x)}{\partial x_6} \\ 0 & 0 & 0 & 0 & 0 & 0 \\ \frac{\partial g_{42}(x)}{\partial x_1} & \frac{\partial g_{42}(x)}{\partial x_2} & \frac{\partial g_{42}(x)}{\partial x_3} & \frac{\partial g_{42}(x)}{\partial x_4} & \frac{\partial g_{42}(x)}{\partial x_5} & \frac{\partial g_{42}(x)}{\partial x_6} \\ 0 & 0 & 0 & 0 & 0 & 0 \\ \frac{\partial g_{62}(x)}{\partial x_1} & \frac{\partial g_{62}(x)}{\partial x_2} & \frac{\partial g_{62}(x)}{\partial x_3} & \frac{\partial g_{62}(x)}{\partial x_4} & \frac{\partial g_{62}(x)}{\partial x_5} & \frac{\partial g_{62}(x)}{\partial x_6} \end{pmatrix} \tag{44}$$

Computation of the Jacobian matrix $\nabla_x g_3(x) \mid_{(x^*,u^*)}$:

It holds that $g_{23}(x) = \frac{M_{31}}{detM}$ thus for $i = 1, 2, 3, 4, 5, 6$

$$\frac{\partial g_{23}}{\partial x_i} = \frac{\frac{\partial M_{31}}{\partial x_i} detM - M_{31}\frac{\partial detM}{\partial x_i}}{detM^2} \tag{45}$$

Moreover $g_{43}(x) = -\frac{M_{32}}{detM}$ thus for $i = 1, 2, 3, 4, 5, 6$

$$\frac{\partial g_{43}}{\partial x_i} = -\frac{\frac{\partial M_{32}}{\partial x_i} detM - M_{32}\frac{\partial detM}{\partial x_i}}{detM^2} \tag{46}$$

Additionally $g_{63}(x) = \frac{M_{33}}{detM}$ thus for $i = 1, 2, 3, 4, 5, 6$

$$\frac{\partial g_{63}}{\partial x_i} = \frac{\frac{\partial M_{33}}{\partial x_i} detM - M_{33}\frac{\partial detM}{\partial x_i}}{detM^2} \tag{47}$$

Consequently

$$\nabla_x g_3(x) \mid_{(x^*,u^*)} = \begin{pmatrix} 0 & 0 & 0 & 0 & 0 & 0 \\ \frac{\partial g_{23}(x)}{\partial x_1} & \frac{\partial g_{23}(x)}{\partial x_2} & \frac{\partial g_{23}(x)}{\partial x_3} & \frac{\partial g_{23}(x)}{\partial x_4} & \frac{\partial g_{23}(x)}{\partial x_5} & \frac{\partial g_{23}(x)}{\partial x_6} \\ 0 & 0 & 0 & 0 & 0 & 0 \\ \frac{\partial g_{43}(x)}{\partial x_1} & \frac{\partial g_{43}(x)}{\partial x_2} & \frac{\partial g_{43}(x)}{\partial x_3} & \frac{\partial g_{43}(x)}{\partial x_4} & \frac{\partial g_{43}(x)}{\partial x_5} & \frac{\partial g_{43}(x)}{\partial x_6} \\ 0 & 0 & 0 & 0 & 0 & 0 \\ \frac{\partial g_{63}(x)}{\partial x_1} & \frac{\partial g_{63}(x)}{\partial x_2} & \frac{\partial g_{63}(x)}{\partial x_3} & \frac{\partial g_{63}(x)}{\partial x_4} & \frac{\partial g_{63}(x)}{\partial x_5} & \frac{\partial g_{63}(x)}{\partial x_6} \end{pmatrix} \tag{48}$$

Computation of the partial derivatives of the elements of the inertia matrix (a) $\frac{\partial detM}{\partial x_i} = 0$ for $i = 1, 2, 4, 5, 6$ and $\frac{\partial detM}{\partial x_3} = -I_t(I_a + h_z^2)(2I_a + 2mh_z^2)cos(z_3)sin(x_3)$, (b) $\frac{\partial M_{11}}{\partial x_i} = 0$ for $i = 1, 2, 3, 4, 5, 6$, (c) $\frac{\partial M_{12}}{\partial x_i} = 0$ for $i = 1, 2, 3, 4, 5, 6$, (d) $\frac{\partial M_{13}}{\partial x_i} = 0$ for $i = 1, 2, 4, 5, 6$ and $\frac{\partial M_{13}}{\partial x_3} = -(I_t cos(x_3))(I_a + mh_z^2)$, (e) $\frac{\partial M_{21}}{\partial x_i} = 0$ for $i = 1, 2, 3, 4, 5, 6$, (f) $\frac{\partial M_{22}}{\partial x_i} = 0$ for $i = 1, 2, 4, 5, 6$ and $\frac{\partial M_{22}}{\partial x_i} = -(I_a + mh_z^2)I_t cos(x_3)sin(x_3)$, (g) $\frac{\partial M_{23}}{\partial x_i} = 0$ for $i = 1, 2, 3, 4, 5, 6$, (h) $\frac{\partial M_{31}}{\partial x_i} = 0$ for $i = 1, 2, 4, 5, 6$ and $\frac{\partial M_{31}}{\partial x_3} = -(I_a + mh_z^2)I_t cos(x_3)$, (i) $\frac{\partial M_{32}}{\partial x_i} = 0$ for

$i = 1, 2, 3, 4, 5, 6$, (j) $\frac{\partial M_{33}}{\partial x_i} = 0$ for $i = 1, 2, 4, 5, 6$ and $\frac{\partial M_{33}}{\partial x_3} = [-2I_a + 2I_t - 2mh_z^2]cos(x_3)sin(x_3)(I_a + mh_z^2)$

Computation of the partial derivatives of the elements of the Coriolis matrix: (a) $\frac{\partial C_1}{\partial x_1} = 0$, $\frac{\partial C_1}{\partial x_2} = 2x_4cos(x_3)sin(x_3)I_a + 2x_4sin(x_3)cos(x_3)(I_t - mh_z^2)$, $\frac{\partial C_1}{\partial x_3} = 2x_2x_4[-sin(x_3)^2 + cos(x_3)^2]I_a - 2x_2x_4[cos(x_3)^2 - sin(x_3)^2](I_t - mh_z^2) - I_4x_4x_6sin(x_3)$, $\frac{\partial C_1}{\partial x_4} = 2x_2cos(x_3)sin(x_3)I_a + 2x_4sin(x_3)cos(x_3)(I_t - mh_z^2) + I_tx_6cos(x_3)$, $\frac{\partial C_1}{\partial x_5} = 0$, $\frac{\partial C_1}{\partial x_6} = I_tx_4cos(x_3)$,

(b) $\frac{\partial C_2}{\partial x_1} = 0$, $\frac{\partial C_2}{\partial x_2} = 2x_2sin(x_5)cos(x_3)(I_a + mh_z^2 - I_t) - I_tx_6cos()x_3$, $\frac{\partial C_2}{\partial x_3} = -x_2^2sin(x_5)sin(x_3)(I_a + mh_z^2 - I_t) + I_tx_2x_6sin(x_3)$, $\frac{\partial C_2}{\partial x_4} = 0$, $\frac{\partial C_2}{\partial x_5} = -x_2^2sin(x_5)sin(x_3)(I_a + mh_z^2 - I_t)$, $\frac{\partial C_2}{\partial x_6} = 0 - I_tx_2cos(x_3)$,

(c) $\frac{\partial C_3}{\partial x_1} = 0$, $\frac{\partial C_3}{\partial x_2} = I_tx_2cos(x_3)$, $\frac{\partial C_3}{\partial x_3} = I_tx_4cos(x_3)$, $\frac{\partial C_3}{\partial x_4} = 0$, $\frac{\partial C_3}{\partial x_5} = -I_tx_2x_4sin(x_3)$, $\frac{\partial C_3}{\partial x_6} = 0$.

Computation of the partial derivatives of the elements of the gravitational forces vector: (a) $\frac{\partial G_1}{\partial x_1} = -mgh_z[cos(x_3)sin(x_1)]$, $\frac{\partial G_1}{\partial x_2} = 0$, $\frac{\partial G_1}{\partial x_3} = mgh_z[sin(x_3)sin(x_1)]$, $\frac{\partial G_1}{\partial x_4} = 0$, $\frac{\partial G_1}{\partial x_5} = 0$, $\frac{\partial G_1}{\partial x_6} = 0$.

(b) $\frac{\partial G_2}{\partial x_1} = mgh_z[sin(x_3)sin(x_1)]$, $\frac{\partial G_2}{\partial x_2} = 0$, $\frac{\partial G_2}{\partial x_3} = mgh_z[cos(x_3)sin(x_1)]$, $\frac{\partial G_2}{\partial x_4} = 0$, $\frac{\partial G_2}{\partial x_5} = 0$, $\frac{\partial G_2}{\partial x_6} = 0$.

(c) $\frac{\partial G_3}{\partial x_i} = 0$ for $i = 1, 2, \cdots, 6$

Computation of the partial derivatives of the elements of the disturbance torques vector $\frac{\partial \tau_{d1}}{\partial x_i} = 0$ for $i = 1, 3, 4, 5, 6$ and $\frac{\partial \tau_{d1}}{\partial x_2} = b_1 2$, $\frac{\partial \tau_{d2}}{\partial x_i} = 0$ for $i = 1, 2, 3, 5, 6$ and $\frac{\partial \tau_{d2}}{\partial x_4} = b_2$, $\frac{\partial \tau_{d3}}{\partial x_i} = 0$ for $i = 1, 2, 3, 4, 5$ and $\frac{\partial \tau_{d3}}{\partial x_6} = b_6$,

4 Nonlinear optimal controller and stability properties

4.1 Stabilizing feedback control

After linearization around its current operating point, the dynamic model of the permanent magnet synchronous spherical motor, is written as

$$\dot{x} = Ax + Bu + d_1 \tag{49}$$

where A and B are the Jacobian matrices of the nonlinear state-space description of the system. Parameter d_1 stands for the linearization error in the model of the spherical motor, appearing previously in Eq. (49). The reference setpoints for the state vector of the spherical motor are denoted by $\mathbf{x_d} = [x_1^d, \cdots, x_6^d]$. Tracking of this setpoint is achieved after applying the control input u_d. At every time instant the control input u_d is assumed to differ from the control input u appearing in Eq. (49) by an amount equal to Δu, that is $u_d = u + \Delta u$ (Rigatos and Karapanou, 2020)

$$\dot{x}_d = Ax_d + Bu_d + d_2 \tag{50}$$

The kinematics of the controlled system described in Eq. (49) can be also written as

$$\dot{x} = Ax + Bu + Bu_d - Bu_d + d_1 \tag{51}$$

and by denoting $d_3 = -Bu_d + d_1$ as an aggregate disturbance term one obtains

$$\dot{x} = Ax + Bu + Bu_d + d_3 \tag{52}$$

By subtracting Eq. (50) from Eq. (52) one has

$$\dot{x} - \dot{x}_d = A(x - x_d) + Bu + d_3 - d_2 \tag{53}$$

By denoting the tracking error as $e = x - x_d$ and the aggregate disturbance term as $\tilde{d} = d_3 - d_2$, the tracking error dynamics becomes

$$\dot{e} = Ae + Bu + \tilde{d} \tag{54}$$

For the approximately linearized model of the system a stabilizing feedback controller is developed. The controller, follows the optimal (H-infinity) control concept, and has the form

$$u(t) = -Ke(t) \tag{55}$$

with $K = \frac{1}{r}B^T P$ where P is a positive definite symmetric matrix which is obtained from the solution of the Riccati equation (Rigatos and Karapanou, 2020)

$$A^T P + PA + Q - P(\tfrac{2}{r}BB^T - \tfrac{1}{\rho^2}LL^T)P = 0 \tag{56}$$

where Q is a positive semi-definite symmetric matrix. The diagram of the considered control loop is depicted in Fig. 2.

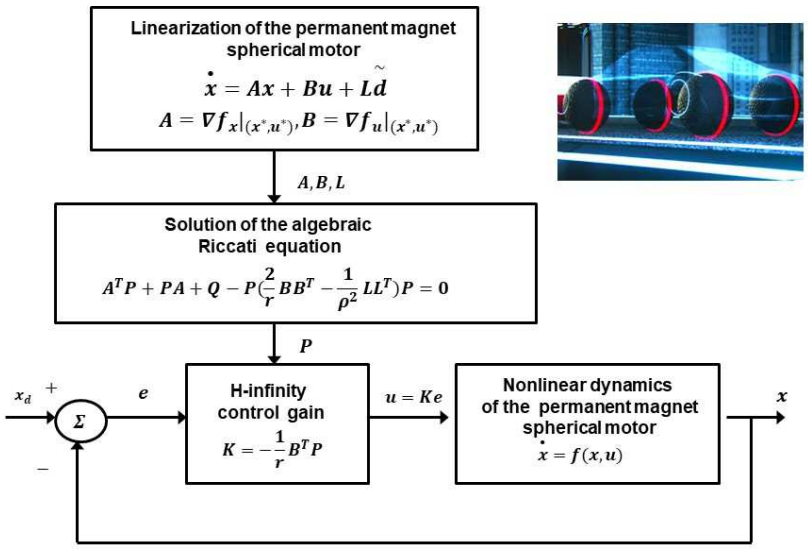

Figure 2: Diagram of the control scheme for the permanent magnet synchronous spherical motor (Source: Authors' own work)

With reference to Eq. (49), the solution of the H-infinity feedback control problem for the permanent magnet spherical motor and the computation of the worst case disturbance that the related controller can sustain, comes from superposition of Bellman's optimality principle when considering that the permanent

magnet spherical motor is affected by two separate inputs (i) the control input u (ii) the cumulative disturbance input $\tilde{d}(t)$. Solving the optimal control problem for u, that is for the minimum variation (optimal) control input that achieves elimination of the state vector's tracking error, gives $u = -\frac{1}{r}B^T Pe$. Equivalently, solving the optimal control problem for $\tilde{d}$, that is for the worst case disturbance that the control loop can sustain gives $\tilde{d} = \frac{1}{\rho^2}L^T Pe$.

4.2 Lyapunov stability analysis

Through Lyapunov stability analysis it will be shown that the proposed nonlinear control scheme assures H_∞ tracking performance for the permanent magnet spherical synchronous motor, and that in case of bounded disturbance terms asymptotic convergence to the reference setpoints is achieved. The tracking error dynamics for the permanent magnet spherical motor is written in the form

$$\dot{e} = Ae + Bu + L\tilde{d} \tag{57}$$

where in the permanent magnet spherical motor's case $L \in R^{6\times 6}$ is the disturbance-inputs gain matrix. Variable $\tilde{d}$ denotes model uncertainties and external disturbances of the permanent magnet spherical motor. The following Lyapunov equation is considered

$$V = \frac{1}{2}e^T Pe \tag{58}$$

where $e = x - x_d$ is the tracking error. By differentiating with respect to time one obtains

$$\begin{gathered}\dot{V} = \frac{1}{2}\dot{e}^T Pe + \frac{1}{2}e^T P\dot{e} \Rightarrow \\ \dot{V} = \frac{1}{2}[Ae + Bu + L\tilde{d}]^T Pe + \frac{1}{2}e^T P[Ae + Bu + L\tilde{d}] \Rightarrow\end{gathered} \tag{59}$$

$$\begin{gathered}\dot{V} = \frac{1}{2}[e^T A^T + u^T B^T + \tilde{d}^T L^T]Pe + \\ + \frac{1}{2}e^T P[Ae + Bu + L\tilde{d}] \Rightarrow\end{gathered} \tag{60}$$

$$\begin{gathered}\dot{V} = \frac{1}{2}e^T A^T Pe + \frac{1}{2}u^T B^T Pe + \frac{1}{2}\tilde{d}^T L^T Pe + \\ \frac{1}{2}e^T PAe + \frac{1}{2}e^T PBu + \frac{1}{2}e^T PL\tilde{d}\end{gathered} \tag{61}$$

The previous equation is rewritten as

$$\begin{gathered}\dot{V} = \frac{1}{2}e^T(A^T P + PA)e + (\frac{1}{2}u^T B^T Pe + \frac{1}{2}e^T PBu) + \\ + (\frac{1}{2}\tilde{d}^T L^T Pe + \frac{1}{2}e^T PL\tilde{d})\end{gathered} \tag{62}$$

Assumption: For given positive definite matrix Q and coefficients r and ρ there exists a positive definite matrix P, which is the solution of the following matrix equation

$$A^T P + PA = -Q + P(\frac{2}{r}BB^T - \frac{1}{\rho^2}LL^T)P \tag{63}$$

Moreover, the following feedback control law is applied to the system

$$u = -\frac{1}{r}B^T Pe \tag{64}$$

By substituting Eq. (63) and Eq. (64) one obtains

$$\begin{gathered}\dot{V} = \frac{1}{2}e^T[-Q + P(\frac{2}{r}BB^T - \frac{1}{\rho^2}LL^T)P]e + \\ + e^T PB(-\frac{1}{r}B^T Pe) + e^T PL\tilde{d} \Rightarrow\end{gathered} \tag{65}$$

$$\begin{gathered}\dot{V} = -\frac{1}{2}e^T Qe + \frac{1}{r}e^T PBB^T Pe - \frac{1}{2\rho^2}e^T PLL^T Pe \\ -\frac{1}{r}e^T PBB^T Pe + e^T PL\tilde{d}\end{gathered} \tag{66}$$

which after intermediate operations gives

$$\dot{V} = -\frac{1}{2}e^T Q e - \frac{1}{2\rho^2}e^T PLL^T Pe + e^T PL\tilde{d} \tag{67}$$

or, equivalently

$$\begin{aligned}\dot{V} = -\frac{1}{2}e^T Q e - \frac{1}{2\rho^2}e^T PLL^T Pe + \\ +\frac{1}{2}e^T PL\tilde{d} + \frac{1}{2}\tilde{d}^T L^T Pe\end{aligned} \tag{68}$$

Lemma: The following inequality holds

$$\frac{1}{2}e^T PL\tilde{d} + \frac{1}{2}\tilde{d}L^T Pe - \frac{1}{2\rho^2}e^T PLL^T Pe \leq \frac{1}{2}\rho^2\tilde{d}^T\tilde{d} \tag{69}$$

Proof: The binomial $(\rho\alpha - \frac{1}{\rho}b)^2$ is considered. Expanding the left part of the above inequality one gets

$$\begin{aligned}\rho^2a^2 + \frac{1}{\rho^2}b^2 - 2ab \geq 0 \Rightarrow \frac{1}{2}\rho^2a^2 + \frac{1}{2\rho^2}b^2 - ab \geq 0 \Rightarrow \\ ab - \frac{1}{2\rho^2}b^2 \leq \frac{1}{2}\rho^2a^2 \Rightarrow \frac{1}{2}ab + \frac{1}{2}ab - \frac{1}{2\rho^2}b^2 \leq \frac{1}{2}\rho^2a^2\end{aligned} \tag{70}$$

The following substitutions are carried out: $a = \tilde{d}$ and $b = e^T PL$ and the previous relation becomes

$$\frac{1}{2}\tilde{d}^T L^T Pe + \frac{1}{2}e^T PL\tilde{d} - \frac{1}{2\rho^2}e^T PLL^T Pe \leq \frac{1}{2}\rho^2\tilde{d}^T\tilde{d} \tag{71}$$

Eq. (71) is substituted in Eq. (68) and the inequality is enforced, thus giving

$$\dot{V} \leq -\frac{1}{2}e^T Q e + \frac{1}{2}\rho^2\tilde{d}^T\tilde{d} \tag{72}$$

Eq. (72) shows that the H_∞ tracking performance criterion is satisfied. The integration of $\dot{V}$ from 0 to T gives

$$\begin{aligned}\int_0^T \dot{V}(t)dt \leq -\frac{1}{2}\int_0^T ||e||_Q^2 dt + \frac{1}{2}\rho^2\int_0^T ||\tilde{d}||^2 dt \Rightarrow \\ 2V(T) + \int_0^T ||e||_Q^2 dt \leq 2V(0) + \rho^2\int_0^T ||\tilde{d}||^2 dt\end{aligned} \tag{73}$$

Moreover, if there exists a positive constant $M_d > 0$ such that

$$\int_0^\infty ||\tilde{d}||^2 dt \leq M_d \tag{74}$$

then one gets

$$\int_0^\infty ||e||_Q^2 dt \leq 2V(0) + \rho^2 M_d \tag{75}$$

Thus, the integral $\int_0^\infty ||e||_Q^2 dt$ is bounded. Moreover, $V(T)$ is bounded and from the definition of the Lyapunov function V in Eq. (58) it becomes clear that $e(t)$ will be also bounded since $e(t) \in \Omega_e = \{e | e^T Pe \leq 2V(0) + \rho^2 M_d\}$. According to the above and with the use of Barbalat's Lemma one obtains $\lim_{t\to\infty} e(t) = 0$.

After following the stages of the stability proof one arrives at Eq. (72) which shows that the H-infinity tracking performance criterion holds. By selecting the attenuation coefficient ρ to be sufficiently small and in particular to satisfy $\rho^2 < ||e||_Q^2 / ||\tilde{d}||^2$ one has that the first derivative of the Lyapunov function is upper bounded by 0. This condition holds at each sampling instance and consequently global stability for the control loop can be concluded.

Comparing to other nonlinear approaches that one could have considered for the dynamic model of the spherical motors the article's nonlinear optimal control method exhibits specific advantages. These are outlined in the following: (i) Compared to global linearization-based techniques such as Lie algebra-based control and flatness-based control through transformation into canonical forms and eigenvalues assignment

the proposed nonlinear optimal control method does not need complicated state-space model transformations with the definition of new state variables (diffeomorphisms). The optimal control is applied directly on the initial nonlinear state space model of the system without involving inverse transformations that may come against singularity issues, (ii) compared to popular approaches for treating the optimal control problem electric motors and actuators, such as Nonlinear Model Predictive Control (NMPC) the proposed nonlinear optimal control method is of proven global stability and its convergence to optimum does not depend on parameter values selection and on initialization (multiple shooting methods), (iii) compared to sliding-mode control the nonlinear optimal control method does not need the controlled system to be found or to be transformed into a specific state-space form. For instance it is known that unless the system is in the input-output linearized form (canonical form) there is no systematic manner for defining sliding surfaces and for computing the sliding-mode control inputs, (iv) compared to backstepping control the nonlinear optimal control method does not need the controlled system to be found or to be transformed into a specific state-space form. For instance in backstepping control unless the system is found in the triangular (strict feedback) form there is no systematic manner to compute the stabilizing feedback control inputs, (v) unlike multiple local-models feedback control the proposed nonlinear optimal control approach does not induce an excessive computational load. It does not need linearization around multiple arbitrarily chosen operating points and does not require the solution of multiple Riccati equations or LMIs (vi) compared to PID-type control, the nonlinear optimal control method does not follow a heuristics-based selection of controller parameters and ensures global stability in changes of operating points and under variable operating conditions.

5 Flatness-based control implemented in successive loops

5.1 A successive loops state-space model

A different formulation is introduced now for the state-space model of the permanent magnet synchronous spherical motor. The state vector of the spherical motor is defined as

$$\begin{aligned} x = [x_1, x_2, x_3, x_4, x_5, x_6]^T \Rightarrow \\ x = [\alpha, \beta, \gamma, \dot{\alpha}, \dot{\beta}, \dot{\gamma}]^T \end{aligned} \tag{76}$$

Consequently, one has that

$$\begin{pmatrix} \dot{x}_1 \\ \dot{x}_2 \\ \dot{x}_3 \\ \dot{x}_4 \\ \dot{x}_5 \\ \dot{x}_6 \end{pmatrix} = \begin{pmatrix} x_4 \\ x_5 \\ x_6 \\ \frac{-M_{11}(C_1+G_1+\tau_{d1})+M_{21}(C_2+G_2+\tilde{d}_2)-M_{31}(C_3+G_3+\tau_{d3})}{detM} \\ \frac{M_{12}(C_1+G_1+\tau_{d1})-M_{22}(C_2+G_2+\tilde{d}_2)+M_{32}(C_3+G_3+\tau_{d3})}{detM} \\ \frac{-M_{13}(C_1+G_1+\tau_{d1})+M_{23}(C_2+G_2+\tilde{d}_2)-M_{33}(C_3+G_3+\tau_{d3})}{detM} \end{pmatrix} + \begin{pmatrix} 0 & 0 & 0 \\ 0 & 0 & 0 \\ 0 & 0 & 0 \\ \frac{M_{11}}{detM} & -\frac{M_{21}}{detM} & \frac{M_{31}}{detM} \\ -\frac{M_{12}}{detM} & \frac{M_{22}}{detM} & -\frac{M_{32}}{detM} \\ \frac{M_{13}}{detM} & -\frac{M_{23}}{detM} & \frac{M_{33}}{detM} \end{pmatrix} \begin{pmatrix} u_1 \\ u_2 \\ u_3 \end{pmatrix} \tag{77}$$

Equivalently, the motor's state-space model is written as follows:

$$\begin{pmatrix}\dot{x}_1\\ \dot{x}_2\\ \dot{x}_3\\ \dot{x}_4\\ \dot{x}_5\\ \dot{x}_6\end{pmatrix}=\begin{pmatrix}x_4\\ x_5\\ x_6\\ f_4(x)\\ f_5(x)\\ f_6(x)\end{pmatrix}+\begin{pmatrix}0 & 0 & 0\\ 0 & 0 & 0\\ 0 & 0 & 0\\ g_{41}(x) & g_{42}(x) & g_{43}(x)\\ g_{51}(x) & g_{52}(x) & g_{53}(x)\\ g_{61}(x) & g_{62}(x) & g_{63}(x)\end{pmatrix}\begin{pmatrix}u_1\\ u_2\\ u_3\end{pmatrix} \tag{78}$$

Next, the following state vectors are defined $x_{13}=[x_1,x_2,x_3]^T$ and $x_{46}=[x_4,x_5,x_6]^T$. Moreover, the following vectors are defined $f_{13}=[x_4,x_5,x_6]^T$ and $f_{46}=[f_4(x),f_5(x),f_6(x)]^T$. Additionally, one defines the matrices $g_{13}=0_{3\times 3}$ and

$$g_{46}=\begin{pmatrix}g_{41}(x) & g_{42}(x) & g_{43}(x)\\ g_{51}(x) & g_{52}(x) & g_{53}(x)\\ g_{61}(x) & g_{62}(x) & g_{63}(x)\end{pmatrix} \tag{79}$$

Thus, the state-space model of the system comes into the following concise formL

$$\begin{pmatrix}\dot{x}_{13}\\ \dot{x}_{46}\end{pmatrix}=\begin{pmatrix}x_{46}\\ f_{46}(x)\end{pmatrix}+\begin{pmatrix}0_{3\times 3}\\ g_{46}(x_{46})\end{pmatrix}u \tag{80}$$

This is a triangular state-space form for the dynamics of the permanent magnet spherical motor. Equivalently, one has the description of the dynamics of the spherical motor through the following two equations:

$$\dot{x}_{13}=x_{46} \tag{81}$$

$$\dot{x}_{45}=f_{46}(x)+g_{46}(x)u \tag{82}$$

It can be shown that under this new state-space description of Eq. (81) and Eq. (82) the spherical motor is a differentially flat system with flat output $Y=x_{13}$. Indeed, from Eq. (81) one has that

$$x_{46}=\dot{x}_{13}\Rightarrow x_{46}=\dot{Y} \tag{83}$$

Consequently, state variable Y is a differential function of the flat output Y. Besides, from Eq. (82) it holds that

$$\begin{array}{c}u=g_{46}(x)^{-1}[\dot{x}_{46}-f_{46}(x)]\Rightarrow\\ u=g_{46}(Y,\dot{Y})^{-1}[\ddot{Y}-f_{46}(Y,\dot{Y})]\end{array} \tag{84}$$

Consequently, control u is also a differential function of the above-noted flat output $Y=x_{13}$. As a result of the previous analysis the dynamic model of the spherical motor in Eq. (81) and Eq. (82) is differentially flat.

5.2 Design of a stabilizing controller in successive loops

It can be shown that each one of Eq. (81) and Eq. (82) is a differentially flat subsystem.

For the subsystem of Eq. (81) x_{13} is the state vector and x_{46} is viewed as a control inputs vector. Thus x_{46} is a differential function of x_{13} and this subsystem is differentially flat. For the subsystem of Eq. (82), x_{46} is the flat output, x_{13} is viewed as a coefficients vector and control inputs u can be written as differential function of x_{46}. Consequently, this is also a differentially flat subsystem.

For the subsystem of Eq. (81) the setpoint is defined as x_{13}^d and the value of the virtual control input which stabilizes this subsystem is

$$x_{46}^*=\dot{x}_{13}^d-K_1(x_{13}-x_{13}^d) \tag{85}$$

Next, the control input that makes x_{46} converge to the targeted value x_{46}^{*} is

$$u = g_{46}(x)^{-1}[\dot{x}_{46}^{d} - f_{46}(x) - K_2(x_{46} - x_{46}^{d})] \tag{86}$$

By applying Eq. (85) and Eq. (86) into Eq. (81) and Eq.(82) respectively, the tracking error dynamics for the two successive loops becomes

$$\begin{array}{c}(\dot{x}_{13} - \dot{x}_{13}^{d}) + K_1(x_{13} - x_{13}^{d}) = 0 \\ (\dot{x}_{46} - \dot{x}_{46}^{d}) + K_2(x_{46} - x_{46}^{d}) = 0\end{array} \tag{87}$$

Next, by defining the tracking error variables $e_{13} = x_{13} - x_{13}^{d}$ and $e_{46} = x_{45} - x_{46}^{d}$ one has

$$\begin{array}{c}\dot{e}_{13} + K_1 e_{13} = 0 \Rightarrow lim_{t\to\infty} e_{13} = 0 \Rightarrow lim_{t\to\infty} x_{13} = x_{13}^{d} \\ \dot{e}_{46} + K_2 e_{46} = 0 \Rightarrow lim_{t\to\infty} e_{46} = 0 \Rightarrow lim_{t\to\infty} x_{46} = x_{46}^{d}\end{array} \tag{88}$$

Consequently $lim_{r\to\infty} x_i(t) = x_i^{d}(t)$ for $i = 1, 2, \cdots, 6$. The global stability properties of this control scheme can be also proven through Lyapunov analysis. To this end the following Lyapunov function is defined

$$V = \tfrac{1}{2}[e_{13}^{T} e_{13} + e_{46}^{T} e_{46}] \tag{89}$$

By differentiating in time one gets

$$\begin{array}{c}\dot{V} = [e_{13}^{T}\dot{e}_{13} + e_{46}^{T}\dot{e}_{46}] \Rightarrow \dot{V} = e_{13}^{T}[-K_1 e_{13}] + e_{46}^{T}[-K_1 e_{46}] \\ \Rightarrow \dot{V} = -e_{13}^{T} K_1 e_{13} - e_{46}^{T} K_2 e_{46} \Rightarrow \dot{V} < 0\end{array} \tag{90}$$

Then $\dot{V} < 0 \ \forall \ e_{13} \neq 0$ and $e_{46} \neq 0$, while $\dot{V} = 0$ only when $e_{13} = 0$ and $e_{46} = 0$. Therefore, $\dot{V}$ is strictly negative and V is a continuously diminishing function which converges asymptotically to 0.

6 Simulation tests

6.1 Results about nonlinear optimal control of the spherical motor

Results about the use of the nonlinear optimal control method on the dynamic model of the permanent magnet synchronous spherical motor are shown in the following diagrams, given in Fig. 3 to Fig. 10. The values of the model's parameters have been according to (Bai et al., 2022). Indicative values about the parameters of the spherical motor were: $m = 5.0kg$, $h_z = 0.005m$, $g = 10m/sec^2$, $b_i = 0.05$ $i = 1, 2, 3$, $I_a = 0.65kg{\cdot}m^2$, $I_t = 0.50kg{\cdot}m^2$. Indicative values about the parameters of the H-infinity controller were: $r = 0.001$, $\rho = 0.2$, $Q = 0.02{\cdot}I_{6\times 6}$, and $L = 10^{-4}{\cdot}I_{6\times 6}$. It can be observed that the nonlinear optimal control method achieves fast and accurate tracking of reference setpoints by the state-variables of the permanent magnet synchronous spherical motor, while keeping also moderate the variations of the control inputs. It is noted that to implement this nonlinear control method one does not have to measure the entire state vector of the system. It suffices to measure at each sampling instance state variables x_1, x_2, x_4 (rotor's turn angles) while state variables x_4, x_5, x_6 (rotor's angular velocities) can be estimated with the use of a nonlinear observer such as the nonlinear H-infinity Kalman Filter (Rigatos and Karapanou, 2020). The minimization of the control inputs amplitude is meaningful, because it also signifies reduction of the cost and of the energy for achieving the control objectives. .

Parameters r, ρ and Q which appear in Eq. (63). are assigned offline constant values, while the gains vector K is updated at each sampling instance, based on the positive definite and symmetric matrix P which is the solution of the method's algebraic Riccati equation. The tracking accuracy and the transient performance of the control scheme depends on the values of coefficients r, ρ and on the values of the elements of the diagonal matrix Q. Actually, for relatively small values of r one achieves elimination of the state vectors' tracking error. Moreover, for relatively high values of the diagonal elements of matrix Q

one achieves fast convergence the state variables' reference trajectories, Finally the smallest value of the attenuation coefficient ρ that results into a valid solution of the method's Riccati equation in the form of the positive definite and symmetric matrix P, is the one that provides the control loop with maximum robustness.

To elaborate on nonlinear optimal control for the permanent magnet synchronous spherical motor the following Tables are given (i) Table Ia providing results about the accuracy of tracking of setpoints by the state variables of the spherical motor under an exact dynamic model, (ii) Table IIa providing results about the accuracy of tracking of setpoints by the state variables of the spherical motor under a model that is subject to disturbances (for instance change $\Delta\alpha\%$ in the elements of the gravitational vector $G_i,\ i = 1, 2, 3$ of the spherical motor's dynamic model), (iii) Table IIIa providing results about the convergence times of the state variables of the spherical motor's state variables to the associated setpoints (Source: Authors' own work).

Table Ia - Nonlinear optimal control

Tracking RMSE $\times 10^{-3}$ for the spherical motor in the disturbance-free case

	$RMSE_{x_1}$	$RMSE_{x_2}$	$RMSE_{x_3}$	$RMSE_{x_4}$	$RMSE_{x_5}$	$RMSE_{x_6}$
test_1	0.1787	0.0001	0.1357	0.0001	0.0002	0.0001
test_2	0.1893	0.0001	0.0627	0.0001	0.0001	0.0001
test_3	0.1048	0.0129	0.0283	0.0212	0.0596	0.0056
test_4	0.0623	0.0480	0.3583	0.2538	0.1263	0.0340
test_5	0.1049	0.0123	0.0283	0.0212	0.0596	0.0056
test_6	0.1248	0.0163	0.1860	0.0344	0.0435	0.0190
test_7	0.1049	0.0123	0.0283	0.0212	0.0596	0.0056
test_8	0.1559	0.0825	0.3956	0.1945	0.0843	0.0672

Table IIa - Nonlinear optimal control

Tracking RMSE $\times 10^{-3}$ for the spherical motor in the case of disturbances

$\Delta a\%$	$RMSE_{x_1}$	$RMSE_{x_2}$	$RMSE_{x_3}$	$RMSE_{x_4}$	$RMSE_{x_5}$	$RMSE_{x_6}$
0%	0.1787	0.0001	0.1357	0.0001	0.0002	0.0001
10%	0.1966	0.0001	0.1490	0.0001	0.0003	0.0001
20%	0.2144	0.0001	0.1625	0.0001	0.0004	0.0001
30%	0.2341	0.0001	0.1757	0.0001	0.0005	0.0001
40%	0.2499	0.0001	0.1889	0.0001	0.0006	0.0001
50%	0.2677	0.0001	0.2021	0.0001	0.0007	0.0001
60%	0.2855	0.0001	0.2153	0.0001	0.0009	0.0001

Table IIIa - Nonlinear optimal control

Convergence times (sec) of states of the spherical motor

No test	$T_s\ x_1$	$T_s\ x_2$	$T_s\ x_3$	$T_s\ x_4$	$T_s\ x_5$	$T_s\ x_6$
test_1	3.5	3.5	4.0	2.5	3.0	3.0
test_2	4.0	3.5	4.5	2.5	4.0	3.0
test_3	4.0	4.0	4.5	3.0	3.0	3.0
test_4	4.0	4.0	4.5	3.0	3.0	3.0
test_5	3.5	3.5	4.5	2.5	3.0	2.5
test_6	3.5	4.0	3.0	2.5	3.0	2.5
test_7	3.0	3.5	4.0	2.5	2.5	3.0
test_8	3.0	3.0	3.5	3.0	2.5	2.5

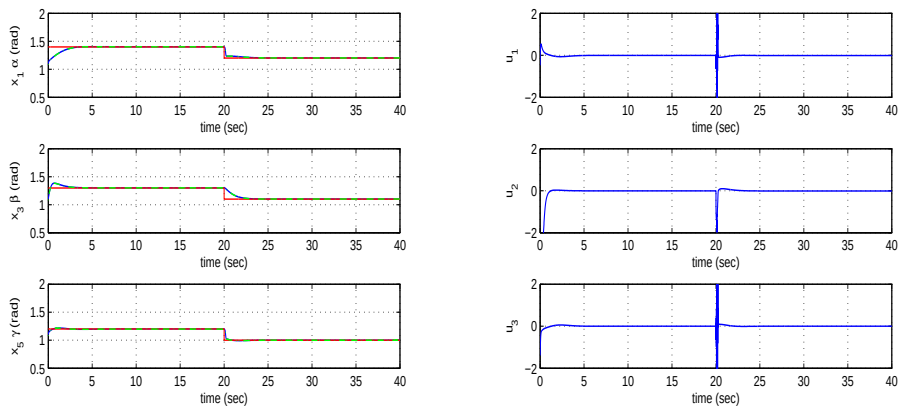

(a) **(b)**

Figure 3: Tracking of setpoint 1 for the permanent magnet synchronous spherical motor with nonlinear optimal control (a) Convergence of the state variables $x_1 = \alpha$, $x_3 = \beta$, $x_5 = \gamma$ (blue lines) to the reference setpoints (red lines) and their KF-based estimation (green line), (b) Variation of the control inputs u_1, u_2 and u_3 (Source: Authors' own work)

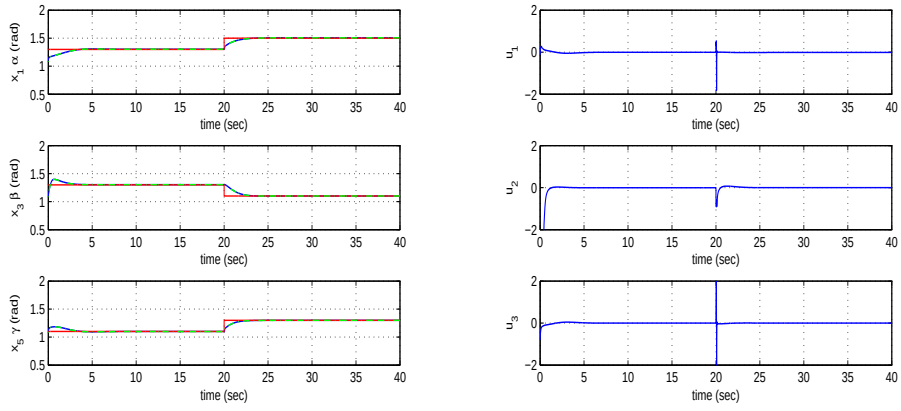

(a) **(b)**

Figure 4: Tracking of setpoint 2 for the permanent magnet synchronous spherical motor with nonlinear optimal control (a) Convergence of the state variables $x_1 = \alpha$, $x_3 = \beta$, $x_5 = \gamma$ (blue lines) to the reference setpoints (red lines) and their KF-based estimation (green line), (b) Variation of the control inputs u_1, u_2 and u_3 (Source: Authors' own work)

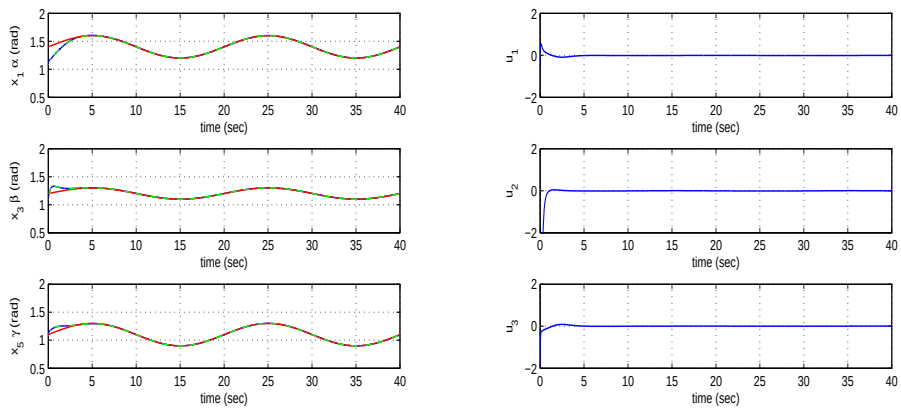

(a) **(b)**

Figure 5: Tracking of setpoint 3 for the permanent magnet synchronous spherical motor with nonlinear optimal control (a) Convergence of the state variables $x_1 = \alpha$, $x_3 = \beta$, $x_5 = \gamma$ (blue lines) to the reference setpoints (red lines) and their KF-based estimation (green line), (b) Variation of the control inputs u_1, u_2 and u_3 (Source: Authors' own work)

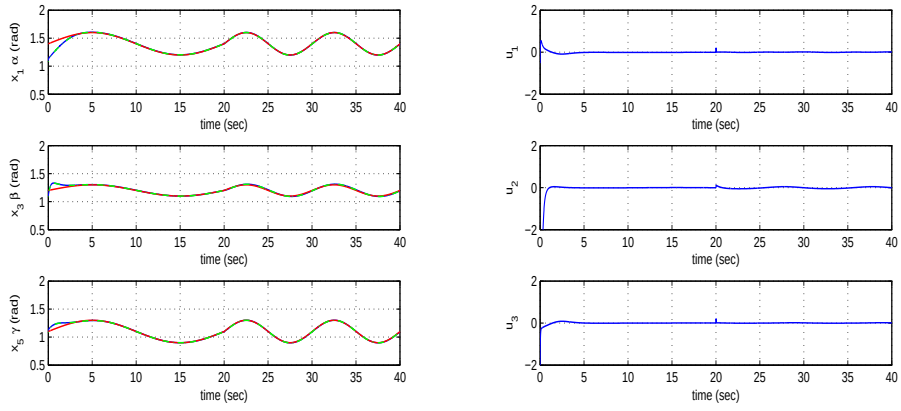

(a) **(b)**

Figure 6: Tracking of setpoint 4 for the permanent magnet synchronous spherical motor with nonlinear optimal control (a) Convergence of the state variables $x_1 = \alpha$, $x_3 = \beta$, $x_5 = \gamma$ (blue lines) to the reference setpoints (red lines) and their KF-based estimation (green line), (b) Variation of the control inputs u_1, u_2 and u_3 (Source: Authors' own work)

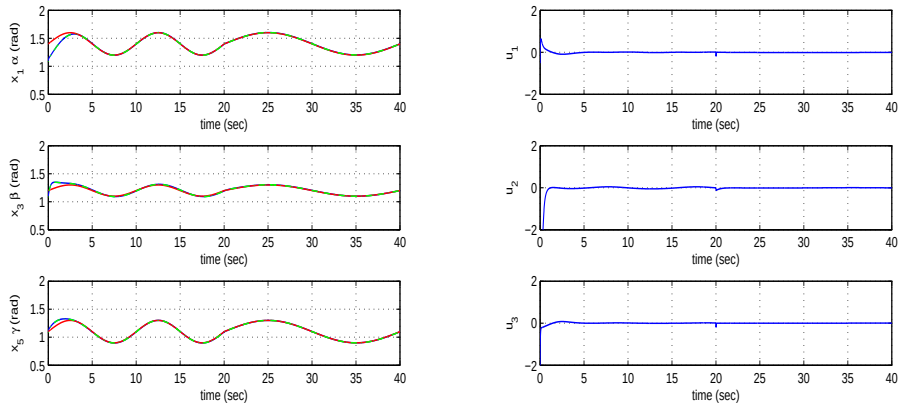

(a) **(b)**

Figure 7: Tracking of setpoint 5 for the permanent magnet synchronous spherical motor with nonlinear optimal control (a) Convergence of the state variables $x_1 = \alpha$, $x_3 = \beta$, $x_5 = \gamma$ (blue lines) to the reference setpoints (red lines) and their KF-based estimation (green line), (b) Variation of the control inputs u_1, u_2 and u_3 (Source: Authors' own work)

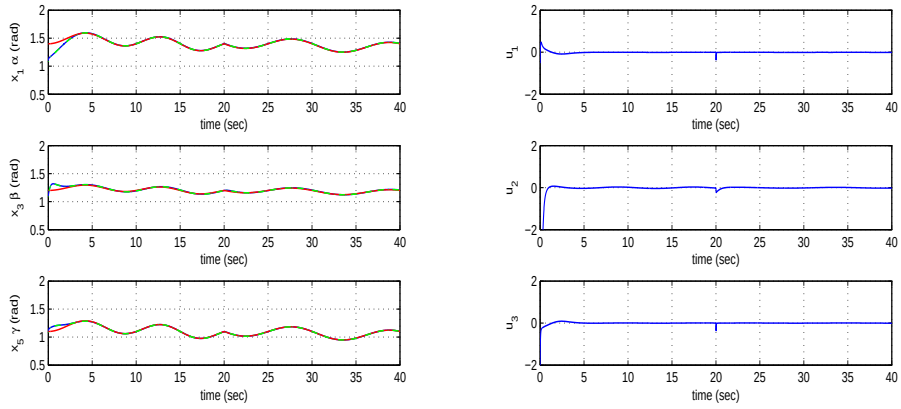

(a) **(b)**

Figure 8: Tracking of setpoint 6 for the permanent magnet synchronous spherical motor with nonlinear optimal control (a) Convergence of the state variables $x_1 = \alpha$, $x_3 = \beta$, $x_5 = \gamma$ (blue lines) to the reference setpoints (red lines) and their KF-based estimation (green line), (b) Variation of the control inputs u_1, u_2 and u_3 (Source: Authors' own work)

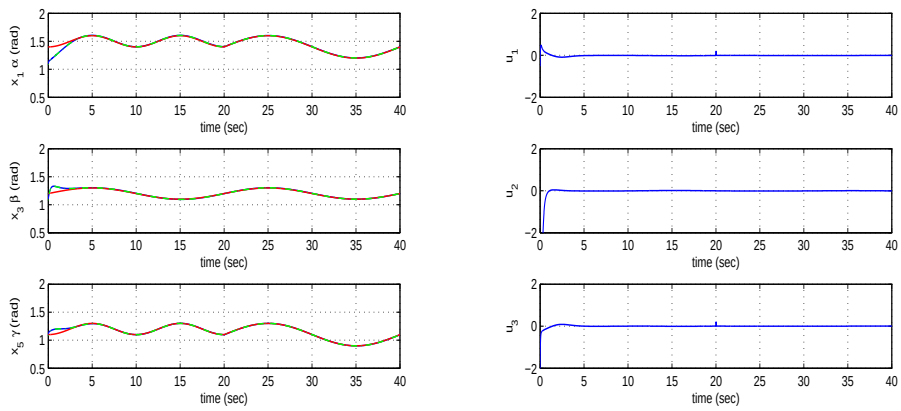

(a) **(b)**

Figure 9: Tracking of setpoint 7 for the permanent magnet synchronous spherical motor with nonlinear optimal control (a) Convergence of the state variables $x_1 = \alpha$, $x_3 = \beta$, $x_5 = \gamma$ (blue lines) to the reference setpoints (red lines) and their KF-based estimation (green line), (b) Variation of the control inputs u_1, u_2 and u_3 (Source: Authors' own work)

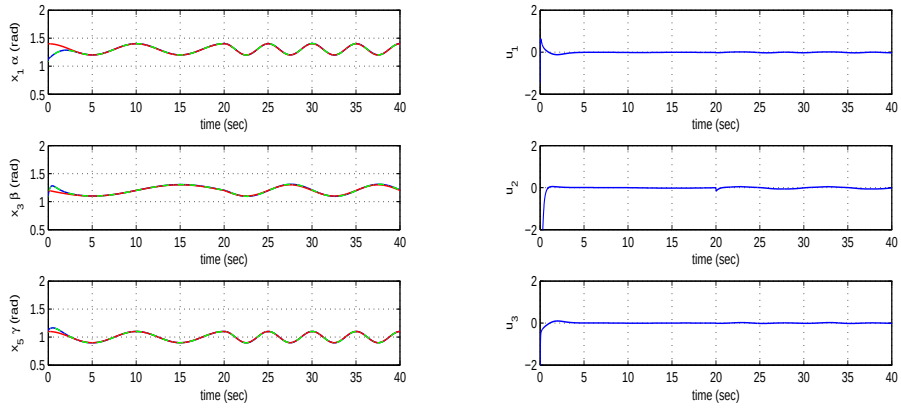

(a) **(b)**

Figure 10: Tracking of setpoint 8 for the permanent magnet synchronous spherical motor with nonlinear optimal control (a) Convergence of the state variables $x_1 = \alpha$, $x_3 = \beta$, $x_5 = \gamma$ (blue lines) to the reference setpoints (red lines) and their KF-based estimation (green line), (b) Variation of the control inputs u_1, u_2 and u_3 (Source: Authors' own work)

6.2 Results about flatness-based control in successive loops of the spherical motor

Results about the use of flatness-based control in successive loops on the dynamic model of the permanent magnet synchronous spherical motor are shown in the following diagrams, given in Fig. 11 to Fig. 18. It can be noticed, that under this control scheme one achieves again fast and precise tracking of reference setpoints for all state variables of the permanent magnet synchronous spherical motor. It is noteworthy, that through the stages of this method one solves also the setpoints definition problem for all state variables of the controlled system. Actually, the selection of setpoints for state variables x_1, x_2 and x_2 is unconstrained. On the other side by defining state variables x_4, x_5 and x_6 as virtual control inputs for the subsystem of x_1, x_2 and x_3 one can find the setpoints for x_4, x_5 and x_6 as functions of the setpoints for x_1, x_2 and x_3. The speed of convergence of the state variables of the permanent magnet synchronous spherical motor under flatness-based control implemented in successive loops depends on the selection of values for the diagonal gain matrices K_1, K_2 of Eq. (85) and Eq. (86). Indicative values for these gain matrices were $K_1 = 0.8 \cdot I_{3\times 3}$ while $K_2 = 2.0 \cdot I_{3\times 3}$.

To elaborate on flatness-based control in successive loops for the permanent magnet synchronous spherical motor the following Tables are given (i) Table Ib providing results about the accuracy of tracking of setpoints by the state variables of the spherical motor under an exact dynamic model, (ii) Table IIb providing results about the accuracy of tracking of setpoints by the state variables of the spherical motor under a model that is subject to disturbances (for instance change $\Delta\alpha\%$ in the elements of the gravitational vector G_i, $i = 1, 2, 3$ of the spherical motor's dynamic model), (iii) Table IIIb providing results about the convergence times of the state variables of the spherical motor's state variables to the associated setpoints (Source: Authors' own work).

Table Ib - Flatness-based control in successive loops

Tracking RMSE $\times 10^{-3}$ for the spherical motor in the disturbance-free case

	$RMSE_{x_1}$	$RMSE_{x_2}$	$RMSE_{x_3}$	$RMSE_{x_4}$	$RMSE_{x_5}$	$RMSE_{x_6}$
test_1	0.1947	0.0214	0.2731	0.0308	0.3515	0.0387
test_2	0.2759	0.0307	0.2731	0.0300	0.4328	0.0476
test_3	0.1729	0.0184	0.3419	0.0372	0.4081	0.0443
test_4	0.1911	0.0263	0.2487	0.0403	0.4237	0.0508
test_5	0.1723	0.0183	0.3410	0.0372	0.4078	0.0442
test_6	0.1834	0.0178	0.3484	0.0371	0.4189	0.0438
test_7	0.1725	0.0184	0.3419	0.0372	0.4677	0.0442
test_8	0.2099	0.0390	0.3585	0.0382	0.4409	0.0589

Table IIb - Flatness-based control in successive loops

Tracking RMSE $\times 10^{-3}$ for the spherical motor in the case of disturbances

$\Delta a\%$	$RMSE_{x_1}$	$RMSE_{x_2}$	$RMSE_{x_3}$	$RMSE_{x_4}$	$RMSE_{x_5}$	$RMSE_{x_6}$
0%	0.1947	0.0214	0.2731	0.0308	0.3515	0.0387
10%	0.2018	0.0096	0.0101	0.0040	0.3211	0.0072
20%	0.2864	0.0130	0.0147	0.0080	0.3238	0.0038
30%	0.5019	0.0119	0.0217	0.0082	0.5880	0.0054
40%	0.7188	0.0101	0.0470	0.0084	0.7844	0.0070
50%	0.8279	0.0103	0.0548	0.0093	0.8819	0.0068
60%	0.9187	0.0106	0.0606	0.0101	0.3641	0.0066

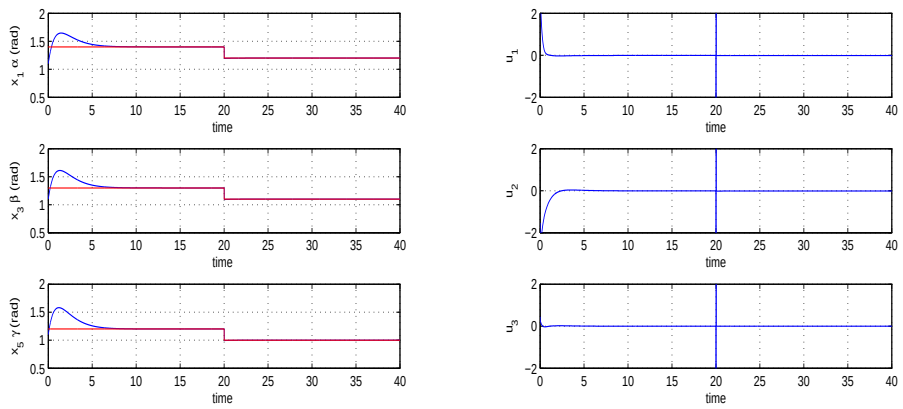

(a) **(b)**

Figure 11: Tracking of setpoint 1 for the permanent magnet synchronous spherical motor with flatness-based control in successive loops (a) Convergence of the state variables $x_1 = \alpha$, $x_3 = \beta$, $x_5 = \gamma$ (blue lines) to the reference setpoints (red lines), (b) Variation of the control inputs u_1, u_2 and u_3 (Source: Authors' own work)

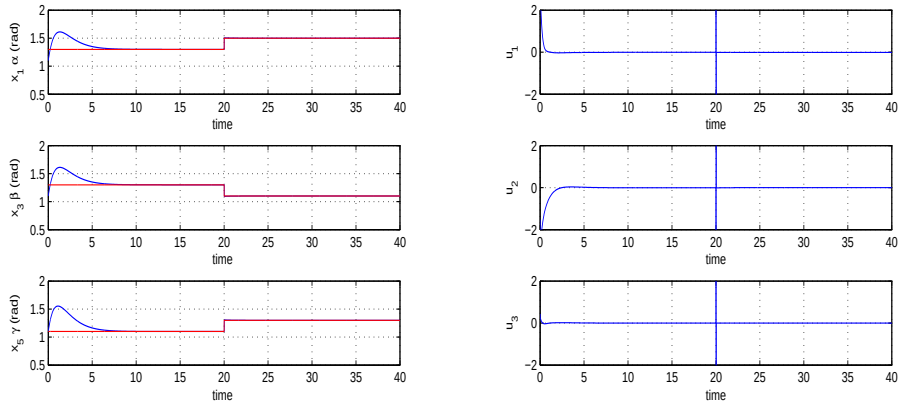

(a) **(b)**

Figure 12: Tracking of setpoint 2 for the permanent magnet synchronous spherical motor with flatness-based control in successive loops (a) Convergence of the state variables $x_1 = \alpha$, $x_3 = \beta$, $x_5 = \gamma$ (blue lines) to the reference setpoints (red lines), (b) Variation of the control inputs u_1, u_2 and u_3 (Source: Authors' own work)

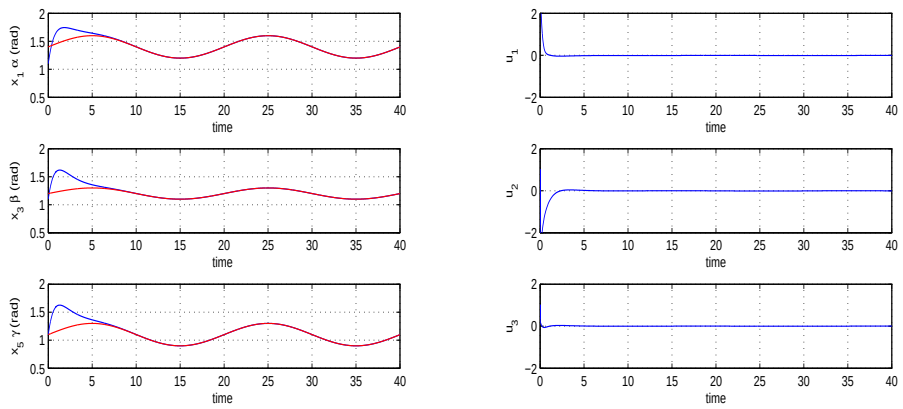

(a) **(b)**

Figure 13: Tracking of setpoint 3 for the permanent magnet synchronous spherical motor with flatness-based control in successive loops (a) Convergence of the state variables $x_1 = \alpha$, $x_3 = \beta$, $x_5 = \gamma$ (blue lines) to the reference setpoints (red lines), (b) Variation of the control inputs u_1, u_2 and u_3 (Source: Authors' own work)

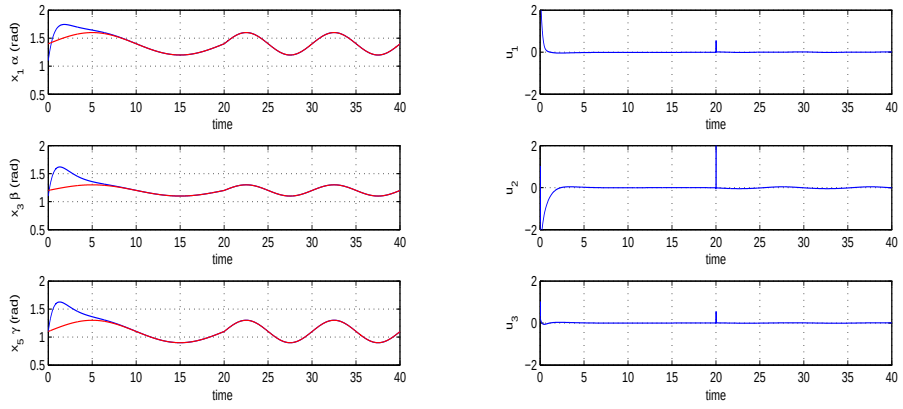

(a) **(b)**

Figure 14: Tracking of setpoint 4 for the permanent magnet synchronous spherical motor with flatness-based control in successive loops (a) Convergence of the state variables $x_1 = \alpha$, $x_3 = \beta$, $x_5 = \gamma$ (blue lines) to the reference setpoints (red lines), (b) Variation of the control inputs u_1, u_2 and u_3 (Source: Authors' own work)

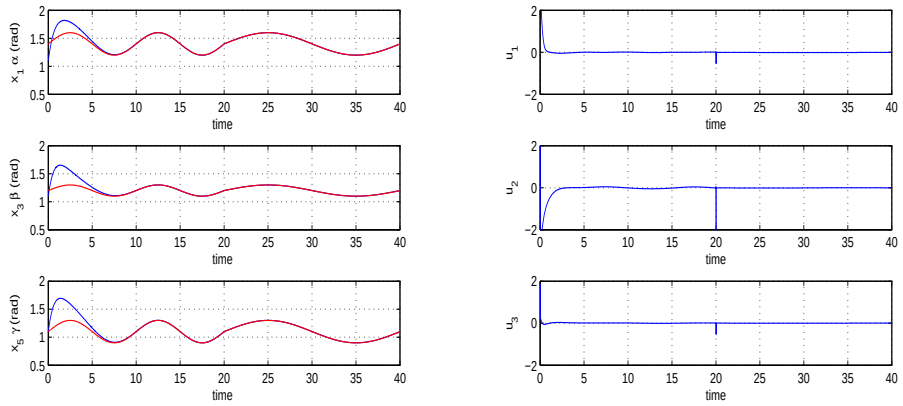

(a) **(b)**

Figure 15: Tracking of setpoint 5 for the permanent magnet synchronous spherical motor with flatness-based control in successive loops (a) Convergence of the state variables $x_1 = \alpha$, $x_3 = \beta$, $x_5 = \gamma$ (blue lines) to the reference setpoints (red lines), (b) Variation of the control inputs u_1, u_2 and u_3 (Source: Authors' own work)

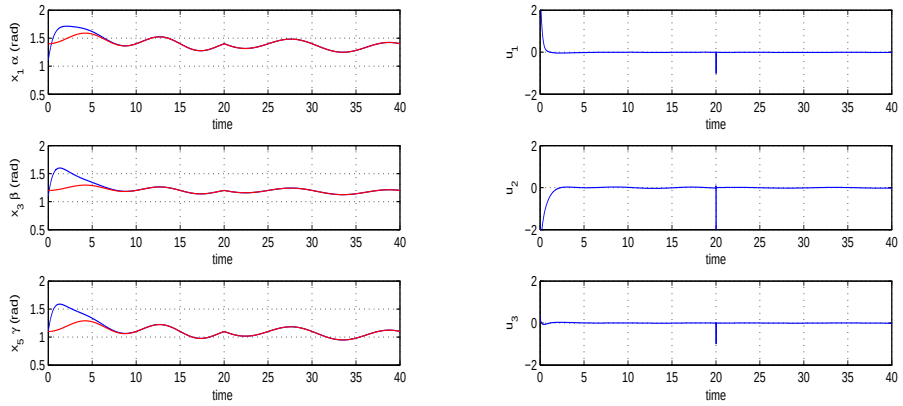

(a) **(b)**

Figure 16: Tracking of setpoint 6 for the permanent magnet synchronous spherical motor with flatness-based control in successive loops (a) Convergence of the state variables $x_1 = \alpha$, $x_3 = \beta$, $x_5 = \gamma$ (blue lines) to the reference setpoints (red lines), (b) Variation of the control inputs u_1, u_2 and u_3 (Source: Authors' own work)

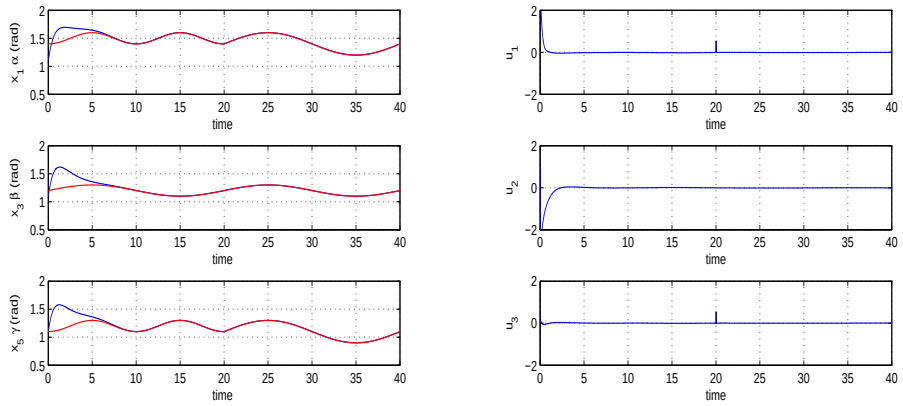

(a) **(b)**

Figure 17: Tracking of setpoint 7 for the permanent magnet synchronous spherical motor with flatness-based control in successive loops (a) Convergence of the state variables $x_1 = \alpha$, $x_3 = \beta$, $x_5 = \gamma$ (blue lines) to the reference setpoints (red lines), (b) Variation of the control inputs u_1, u_2 and u_3 (Source: Authors' own work)

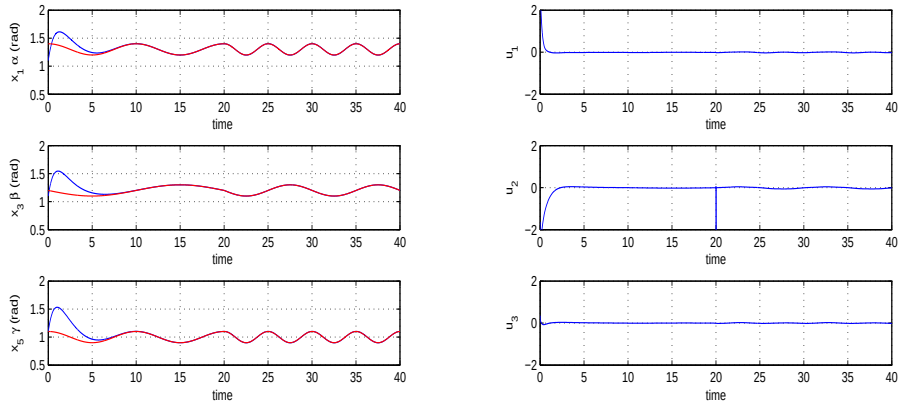

(a) **(b)**

Figure 18: Tracking of setpoint 8 for the permanent magnet synchronous spherical motor with flatness-based control in successive loops (a) Convergence of the state variables $x_1 = \alpha$, $x_3 = \beta$, $x_5 = \gamma$ (blue lines) to the reference setpoints (red lines), (b) Variation of the control inputs u_1, u_2 and u_3 (Source: Authors' own work)

Table IIIb - Flatness-based control in successive loops						
Convergence times (sec) of states of the spherical motor						
No test	$T_s\ x_1$	$T_s\ x_2$	$T_s\ x_3$	$T_s\ x_4$	$T_s\ x_5$	$T_s\ x_6$
$test_1$	7.5	1.0	7.5	1.0	7.5	1.0
$test_2$	7.5	1.0	7.5	1.0	7.5	1.0
$test_3$	7.5	6.0	7.5	6.0	7.5	6.0
$test_4$	7.5	6.0	7.5	6.0	7.5	6.0
$test_5$	7.0	5.0	7.5	5.0	7.0	5.0
$test_6$	7.0	6.0	7.5	6.0	7.0	6.0
$test_7$	6.0	6.0	7.0	6.0	7.5	6.0
$test_8$	6.0	6.0	7.0	6.0	7.0	6.0

7 Conclusions

Permanent magnet synchronous spherical motors find use is several applications, as for instance in manufacturing processes, in actuation of robotic systems and in electric traction systems. Unlike conventional electric motors, in spherical motors the stator is a fixed inner shell while the rotor is a turning outer shell. The torques that generate the turn motion of spherical motors come from the interaction of the stator's EMs with the rotor's PMs. Due to the nonlinear and multivariable structure of the state-space model of spherical motors the solution of the associated nonlinear control problem is a non-trivial task. In this article a novel nonlinear optimal (H-infinity) control approach has been proposed first for the dynamic model of permanent magnet synchronous spherical motors. The method is based on approximate linearization of the motor's state-space model with the use of first-order Taylor series expansion and through the computation of the associated Jacobian matrices. The linearization process takes place at each sampling instance around a temporary operating point which is defined by the present value of the motor's state vector and by the last sampled value of the motor's control inputs vector. To compute the stabilizing feedback gains of this controller an algebraic Riccati equation is repetitively solved at each time-step of the control algorithm. The global stability properties of the control scheme are proven through Lyapunov analysis.

Furthermore, the article has introduced a different solution to the nonlinear control problem of the permanent magnet synchronous spherical motor which is based on flatness-based control implemented in successive loops. It has been proven that the dynamic model of the spherical motor is a differentially flat system. Besides, the state-space model of the system has been decomposed in two subsystems, where the first subsystem has as state vector the turn angles of the rotor while the second subsystem has as state vector the angular velocities of the rotor. Moreover, the first subsystem receives as virtual control inputs vector the angular velocities of the rotor while the second subsystem receives as control inputs the mechanical torques which are generated by the variations of the currents of the stator's EMs. It is shown that each one of these subsystems is differentially flat. This signifies, that a stabilizing feedback controller can be designed by each one of them using the controller design process which is followed for input-output linearizable differentially flat systems. The two subsystems are connected in successive loops and actually the control inputs of the first subsystem become setpoints for the second subsystem. The integrated system which is obtained by connecting the above noted subsystems in cascading mode is globally asymptotically stable and this is proven through Lyapunov analysis. Both control methods have achieved fast and accurate tracking of reference setpoints under moderate variations o of the control inputs.

The two control approaches which have presented in this article, that is nonlinear optimal control and flatness-based control in successive loops, achieve control and stabilization of the nonlinear dynamics of the permanent magnet synchronous spherical motor without changes of state variables and without complicated transformations of the system's state-space model. The first control method is optimal because apart from elimination of the tracking error for the state variables of the spherical motor it also achieves minimization of the variations of the control inputs. By reducing the control inputs' amplitude it en-

sures minimal dispersion of energy by the control loop. The second control method is suboptimal since its objective is only the elimination of the state vectors' tracking error, while the feedback gains of the flatness-based controller in successive loops do not necessarily ensure suppression of the amplitude of the control inputs. Although the flatness-based control method may spend some more energy towards achieving the control objectives it also results in smooth convergence of the state variables to the associated setpoints.

References

Bai K. and Lee K.M. (2014). Direct field-feedback control of a ball joint-like permanent magnet spherical motor. IEEE/ASME Transactions on Mechatronics, 19(3): 976-987.

Bai K., Lee K.M. and Lu J. (2016). A magnetic flux model-based method for detecting multi-DOF motion of a permanent magnet spherical motor. Mechatronics, Elsevier, 39: 217-225.

Bai K. and Lee K.M. (2018). Permanent magnet spherical motors model and field-based approaches for design, testing and control. Springer, 1st Edition.

Bai K., Yan H. and Lee K.M. (2021). Robust control of a spherical motor in moving frame. Mechatronics, Elsevier, 75: 102548-102556.

Bai K., Chen W., Lee K.M., Que Z. and Huang R. (2022). Spherical wrist with hybrid motion-impendance control for enhanced robotic manipulator. IEEE Transactions on Robotics, 38(2): 1174-1184.

Bai K., Ding Y., Que Z., Yan H., Chen X., Wen S. and Lee K.M. (2022). Regulation and tracking control of omnidirectional rotation for spherical motors. IEEE Transactions on Industrial Electronics, 70(2): 1696-1705.

Basseville M. and Nikiforov I. (1993). Detection of abrupt changes: Theory and Applications, Prentice-Hall, New Jersey, USA.

Chai F., Gen L. and Chen L. (2020). A novel tiered-type permanent magnet spherical motor and its rotor orientation measurement principles. IEEE Access, 8: 15303-15312.

Chen W., Zhang L., Yan L. and Lieu J. (2016). Design and control of a three-degrees of freedom permanent magnet spherical actuator. Sensors and Actuators A: Physical, Elsevier, 180: 75-86.

Chen Q., Yang X., Zhang G., Zeng B., Zhuo S., Cao J., Zeng G. and Li Z. (2020). Analytical calculation of magnetic field of double-stator permanent magnet spherical motor considering cogging effect and edge effect, IET Electric Power Applications, 1-20.

Gan L., Pei Y. and Chai P. (2020). Tilting torque calculation of a novel tiered type permanent magnet spherical motor. IEEE Tranactions on Industrial Electronics, 67(1): 421-431.

Guidan L., Haike L. and Bin L. (2011). Spacecraft attitude maneuver control using two parallel mounted 3-DOF spherical actuators. Chinese Journal of Aeronautics, Elsevier, 30(9): 419-425.

Guo X., Li S., Wang Q., Wen Y. and Gang N. (2019). Dynamic analysis and current calculation of a permanent magnet spherical motor for point-to-point motion. IET Electric Power Applications, 13(4): 426-494.

Guo X., Pun K., Wang Q. and Wen Y. (2020). Robust adaptive sliding-mode control of a permanent magnet spherical actuator with delay compensation. IEEE Access, 8: 128096-128105.

Han Z., Liu Z., Meurer T. and He W. (2022). Robust fault-tolerant control of wave equation without estimations of plant anf failure parameters. IFAC 4th Workshop on Control of Systems Governed by Partial Differential Equations, CPDE 2022, Kiel, Germany.

Huang H., He W., Wang J., Zhang L. and Fu Q. (2022). An all-servo drive flapping wing aerial robot capable of autonomous flight. IEEE ASME Transactions on Mechatronics, 27(4): 5484-5494.

Kumagoi M. and Hollis R.L. (2013). Development and control of a 3-DOF spherical induction motor. IEEE ICRA 2013, IEEE 2013 Intl. Conference on Robotics and Automation, Karlsruhe, Germany.

Lee K.M. and Sun H. (2005). Torque model of design and control of a spherical wheel motor. IEEE 2005 Conference on Advanced Intelligent Mechatronics, Monterey, California, USA.

Lee S. and Sun H. (2023). Six-steps commutations torques and desing characteristics of spherical brushless direct current motor. IEEE Transactions on Industrial Electronics, 1-9.

Li X., Liu J., Chen W. and Bai S. (2018). Integrated design, modeling and analysis of a novel spherical motion generator driven by electromagnetic principles. Robotics and Autonomous Systems, Elsevier, 106: 69-81.

Li X., Bai S. and Madsen O. (2019). Dynamic modelling and trajectory tracking control of an electromagnetic direct driven spherical motion generator. Robotics and Computer Integrated Manufacturing, Elsevier, 59: 201-212.

Li H., Zhao Y., Li B., Li G. and Cui L. (2020). Torque calculation of permanent magnet spherical motor based on virtual work method. IEEE Transactions on Industrial Electronics, 67(9): 7735-7745.

Liu J., Ding H., Chen W., and Bai S. (2017). Robust dynamic decoupling control for permanent magnet spherical actuators based on Extended State Observer. IET Control Theory and Applications, 11(5):619-631.

Liu J., Deng H., Hu C., Huo Z. and Chen W. (2017). Adaptive backstepping sliding-mode control for a 3-DOF permanent magnet spherical actuator. Journal of Aerospace Science and Technology, Elsevier, 67: 62-71.

Liu J., Lu X., Cai S., Chen W. and Bai S. (2018). Adaptive fuzzy sliding-mode algorithm-based decentralized control for a permanent magnet spherical actuator. Journal of Systems Science, Taylor and Francis, 50(2): 403-418.

Ogulmuz A.S. and Tirkir M. (2023). Development and performance analysis of novel design 3-DOF non-integrated runner permanent magnet spherical motor,. Engineering Science and Technoology, Elsevier, 40: 101380-101388.

Park J., Kim M., Jang H.G., Jung D.Y. and Park J.M. (2018). Design and control of a permanent magnet spherical wheel motor. ETRI Journal, J. Wiley, 41(6): 838-849.

Rigatos G.G. and Tzafestas S.G. (2007). Extended Kalman Filtering for Fuzzy Modelling and Multi-Sensor Fusion. Mathematical and Computer Modelling of Dynamical Systems, Taylor & Francis, 13: 251-266.

Rigatos G. and Zhang Q. (2009). Fuzzy model validation using the local statistical approach. Fuzzy Sets and Systems, Elsevier, 60(7): 882-904.

Rigatos G.(2015). Nonlinear control and filtering using differential flatness approaches: Applications to electromechanical systems. Springer, Cham, Switzerland.

Rigatos G. (2015). Flatness-based embedded control in successive loops for spark ignited engines. Journal of Physics, IOP Publications, Conference Series No 659, 012019, IFAC ACD 2015, Proc. of the 12th European Workshop on Advanced Control and Diagnosis.

Rigatos G., Siano P. and Cecati C. (2015). A new nonlinear H-infinity feedback control approach for three-phase voltage source converters. Electric Power Components and Systems, Taylor and Francis, 44(3): 302-312.

Rigatos G. (2016). Intelligent Renewable Energy Systems: Modelling and Control. Springer, Cham, Switzerland.

Rigatos G. and Busawon K. (2018). Robotic manipulators and vehicles: Control, estimation and filtering. Springer.

Rigatos G., Siano P., Ademi S. and Wira P. (2018). Flatness-based control of DC-DC converters implemented in successive loops. Electric Power Components and Systems, Taylor and Francis, 46(6): 673-687.

Rigatos G. and Karapanou E. (2020). Advances in applied nonlinear optimal control. Cambridge Scholars Publishing, Newcastle, UK.

Rigatos G., Abbaszadeh M. and Siano P. (2022). Control and estimation of dynamical nonlinear and partial differential equation systems: Theory and applications. IET Publications, London, UK.

Rong Y.. Wang Q., Lu S., Li G., Lu Y. and Xu J. (2019). Improving attitude detection performance for spherical motors using a MEMS inertial measurement sensor. IET Electric Power Applications, 13(2): 198-205.

Rossini L., Chetelier O., Omillon E. and Perriard Y. (2013). Force and torque analytical model of a reaction sphere actuator based on a spherical harmonic rotation and decomposition. IEEE Transactions on Mechatronics, 18(5): 1006-1015.

Sun H. and Lee K.M. (2014). Control system design and input shape for orientation of spherical wheel motors. Control Engineering Practice, Elsevier, 24: 120-129.

Toussaint G.J., Basar T. and Bullo F. (2000). H_∞ optimal tracking control techniques for nonlinear underactuated systems. Proc. IEEE CDC 2000, 39th IEEE Conference on Decision and Control, Sydney Australia.

Wang Y., Fujimoto H. and Hara S. (2016). Torque distribution-based range extension control system for longitudinal motion of electric vehicles by LTI modeling with generalized frequency variable. IEEE/ASME Transactions on Mechatronics, 21(1): 443-452.

Wen Y., Li G., Wang G., Guo X. and Cao W. (2021). Modeling and analysis of permanent magnet spherical motors by a multi-task Gaussian process method and finite element method for output torque. IEEE Transactions on Industrial Electronics, 68(9): 8540-8549.

Wen Y., Liu Z., Wang Q. and Li Q. (2022). Continuous non-singular terminal sliding-mode control of permanent magnet spherical actuator for trajectory tracking based on a modified nonlinear disturbance observer. IET Electric Power Applications, 16(10): 1169-1188.

Wen S., Ding Y., Wu X. and Bai K. (2023). Kinematic analysis and robust control of a spherical-motor-based visual tracking system. IEEE ASME Transactions on Mechatronics, 1-9.

Xia C., Guo C. and Shin T. (2010). A neural network indentifier and fuzzy controller-based algorithm for dynamic decoupling control of permanent magnet spherical motor. IEEE Transactions on Industrial Electronics, 57(8): 2868-2878.

Yan L., Meng-Chen I., Yang G. and Lee K.M. (2006). Analytical and experimental investigation of the magnetic field and torque of a permanent magnet spherical actuator. IEEE Transactions on Mechatronics, 11(4): 409-420.

Yan L., Ming-Chen I., Son H., Lim C.K. and Yang G. (2010). Analysis of pole configuration of permanent magnet spherical actuators. IEEE Transactions on Mechatronics, 15(6): 985-990.

Yan L., Ming-Chen I., Liu C.K. and Lee K.M. (2014). Design and analysis of a permanent magnet spherical actuator. IEEE Transactions on Mechatronics, 11(2): 239-249.

Zhang L., Chen W., Liu J. and Wen Q. (2016). A robust adaptive iterative learning control for trajectory tracking of a permanent magnet spherical actuator. IEEE Transactions on Industrial Electronics, 83(1): 291-301.

Zhao S., Che Y. and Li H. (2023). Three-dimenstional internal identification of Permanent Magnet Spherical Motor based on improved neural network. Journal of Electrical Engineering and Technology, Springer.

Zhou S., Li G., Wang Q., Xu J., Ye Q. and Gao S. (2023). Rotor attitude estimation for spherical motors using multi-agent Kalman XCF algorithm in monocular vision. IEEE Transactions on Industrial Electronics, 70(1): 265-275.

Journal of Robotic Intelligence and Automation

Paper No: RIA-03-23-0032R2

Title: Nonlinear optimal control for permanent magnet synchronous spherical motors

Reply to Editor:

1. *Editor's comment*: At this stage, I would like you to improve/correct the following aspects: Format, English grammar, References, Figures, Figure copyright.

Author's reply: The article has been provisionally accepted for publication and through this additional revision round the following minor issues have been re-checked and addressed: (i) Format: it has been confirmed that the article follows the designated structure and format, (ii) English grammar: the manuscript has been re-checked for typos and the flawless use of English in it has been confirmed, (iii) References: the bibliographic references of the article and the inline citations have been re-edited following Harvard's referencing style, (iv) Figures: It has been confirmed that all figures and Tables appearing in the manuscript are the authors' own work, (v) Figure copyright: It has been confirmed that no copyright issues exist for the figures of the article and that all figures belong exclusively to the authors of the article. The authors believe that after the above-noted re-processing of the article their manuscript has come to a final journal publishable form.